Andreas Kruschitz, BSc.

Particle Surface, What is its Importance on DPI Product Performance?

MASTER'S THESIS

to achieve the university degree of

Diplom-Ingenieur

Master's degree programme: Chemical and Pharmaceutical Engineering

submitted to

Graz University of Technology

Supervisor

Univ.-Prof. Dr.phil.-nat. Sven Stegemann

Institute for Process and Particle Engineering, Technical University, Graz
Research Center Pharmaceutical Engineering GmbH (RCPE), Graz

Dipl.-Ing. Sandra Stranzinger
Research Center Pharmaceutical Engineering GmbH (RCPE), Graz

Graz, November 2017

AFFIDAVIT / EIDESSTATTLICHE ERKLÄRUNG

I declare that I have authored this thesis independently, that I have not used other than the declared sources/resources, and that I have explicitly indicated all material which has been quoted either literally or by content from the sources used. The text document uploaded to TUGRAZonline is identical to the present master‘s thesis.

Ich erkläre an Eides statt, dass ich die vorliegende Arbeit selbstständig verfasst, andere als die angegebenen Quellen/Hilfsmittel nicht benutzt, und die den benutzten Quellen wörtlich und inhaltlich entnommenen Stellen als solche kenntlich gemacht habe. Das in TUGRAZonline hochgeladene Textdokument ist mit der vorliegenden Masterarbeit identisch.

Date/Datum	Signature/Unterschrift

Acknowledgements

The execution of this master thesis would not be possible without the support of some people; therefore, I want to express my gratitude to all of you.

First, I would like to say thank you to Prof. Sven Stegemann for his great support and the supervision of my master thesis. Thank you for the good cooperation.

Special thanks go out to you, Sandra, Joana and Eva. I was always grateful for your scientific advice and I always appreciated your support, your honest feedbacks and the numerous discussions we had.

My thanks also go to Thomas Wutscher and to the whole laboratory and chroma team of the RCPE, who supported me during my experimental tasks.

I also want to say thank you to my friends, who always distracted me from my university work and made my life much easier.

Last but not least I am grateful to have such a gorgeous family. Without your support it would not be possible to accomplish my studies in that way. A special thanks goes to my parents who always trusted and believed in me.

Abstract

Pulmonary drug administration is gaining increasingly importance due to some crucial advantages compared to other routs of drug administration, like a rapid onset of action or avoidance of the first pass effect. Hence, nowadays a great deal of effort is put in the development of systemically acting compounds that are delivered in high doses through the lung. This development of high dosed dry powder inhaler (DPI) formulations is, however, challenging and needs a science based approach to discover influencing factors, affecting DPI performance. Therefore, the aim of this thesis was to examine the impact of jet milled (JM) and spray dried (SD) Salbutamol Sulphate (SS), as model API, on the adhesive mixing with Lactohale 100, on capsule filling and on in vitro aerodynamic performance, when used in high (10%) and in low load (1%). With the two different engineering techniques, SS particles were produced that varied in solid state, particle size and morphology. After particle engineering, a mixing strategy for a tumbling blender was developed, which proved to be suitable to produce homogeneous blends when JM SS was mixed with Lactohale 100 but inappropriate when SD SS was used. The powder bulk properties of the produced blends were then tested with a powder rheometer (FT4). The subsequent capsule filling was performed with a lab scale capsule filling machine, applying the dosator principle. The blends were filled at two different compression ratios (1:2 & 1:4) to find out how the powder bed height affect the capsule fill weight. Simultaneously it was determined how capsule fill weight varied over a filling period of 30 min. The results showed that both the compression ratio and the API load influenced the capsule fill weight. An enhancement of those two parameters led to a higher fill weight. Finally, the aerodynamic performance of the individual blends was tested with a Next Generation Impactor. It turned out that for JM SS blends, higher powder beds and a higher API load by tendency resulted in a higher fine particle fraction (FPF), while for SD SS blends only higher API loads led to a higher FPF. Overall, JM SS blends exhibited in total higher FPFs compared to SD SS blends. The best performance was achieved with the high API load JM SS blend filled at a compression ratio of 1:4 (FPF = 62.82%). For SD SS the best performance was obtained for the high API load blend filled at a compression ratio of 1:2 (FPF = 21.58%).

Kurzfassung

Pulmonale Arzneimittelverabreichung gewinnt immer mehr an Bedeutung für die Behandlung respiratorischer Erkrankungen aufgrund einiger entscheidender Vorteile gegenüber anderer Wege der Arzneimittelverabreichung, wie z.B. ein schnelles Eintreten der Wirkung oder eine Vermeidung des hepatischen First-pass-Effekt. Deswegen wird heutzutage viel Aufwand in die Forschung im Bereich der Entwicklung optimierter Pulvermischungen für Inhalationszwecke gesteckt, die auch die Abgabe hoher Dosen über die Lunge ermöglichen, wie es etwa zur Behandlung Zystischer Fibrose notwendig ist. Diese Entwicklung von hoch dosierten Dry Powder Inhaler (DPI) Formulierungen ist jedoch anspruchsvoll und braucht eine wissenschaftlich-basierte Herangehensweise um entscheidende Faktoren interaktiver Pulvermischungen zu ermitteln, die die in-vivo Arzneimitteldeposition in der Lunge beeinflussen. Deswegen war das Ziel dieser Diplomarbeit den Einfluss von Jet-gemahlenem (JM) und sprüh-getrocknetem (SD) Salbutamol Sulfat (SS) auf das Mischen mit Lactohale 100, das Kapsel-Füllen und auf die in vitro Inhalationsperformance zu untersuchen. Untersucht wurden einerseits eine hohe (10%) und andererseits eine niedrige (1%) Arzneimittelkonzentration in der Pulvermischung. Die SS Partikel, die mit den zwei verschiedenen Techniken produziert wurden, unterschieden sich in ihrer festen Phase, Partikelgröße und Morphologie. Nachdem die Partikel erzeugt wurden, wurde eine Mischstrategie entwickelt, die wie sich herausstellte geeignet war, um homogene Mischungen herzustellen, wenn JM SS mit Lactohale 100 vermischt wurde, aber ungeeignet wenn SD SS verwendet wurde. Von den produzierten Mischungen wurden dann die Pulvereigenschaften mit Hilfe eines Pulver-Rheometers (FT4) untersucht. Das anschließende Kapsel-Füllen wurde mit einer Kapselfüllmaschine im Labormaßstab durchgeführt, die das Dosator-Prinzip verwendet. Die Mischungen wurden bei zwei verschiedenen Verdichtungsverhältnissen (1:2 & 1:4) abgefüllt, um unter anderem herauszufinden wie sich die Pulverbetthöhe auf die Kapselfüllgewichte auswirkt. Gleichzeitig wurde untersucht wie sich die Kapselfüllgewichte über eine Füllperiode von 30 min. verändern. Die Ergebnisse haben gezeigt, dass sowohl das Verdichtungsverhältnis als auch die Menge an Wirkstoff die Kapselfüllgewichte beeinflussen. Eine Erhöhung dieser beiden Parameter führte zu höheren Füllgewichten. Abschließend wurde die Inhalationsperformance der einzelnen Mischungen mit einem “Next Generation Impactor“ geprüft. Es hat sich herausgestellt, dass für die Mischungen mit JM SS, eine Erhöhung der Pulverbetthöhe und der Arzneistoffmenge, tendenziell zu einem höheren Feinpartikelanteil führte. Während für Mischungen mit SD SS nur eine höhere Arzneimittelmenge zu einem höheren Feinpartikelanteil führte. Insgesamt wiesen die Mischungen mit JM SS einen höhere Feinpartikelanteil (FPF) auf als die Mischungen mit SD SS. Die beste

Inhalationsperformance erzielte die Mischung mit dem 10% Anteil an JM SS, abgefüllt bei einem Verdichtungsverhältnis von 1:4 (FPF = 62,82%). Für das SD SS wurde die beste Inhalationsperformance für die Mischung mit einem Wirkstoffanteil von 10%, abgefüllt bei einem Verdichtungsverhältnis von 1:2 (FPF = 21,58%) erreicht.

Table of content

1. Introduction

Pulmonary administration is a traditional way to deliver drug substances in form of aerosol and vapour to the lung in order to achieve a therapeutic effect [1]; providing good opportunity to treat respiratory diseases such as chronically obstructive pulmonary disease (COPD), asthma or cystic fibrosis [2]. Hence, nowadays a great deal of effort has been put on the development of compounds that act not only locally (in the lung) but also systemically, such as protein structures based compounds. Compared to other routes of administration, delivery to the lungs presents some significant advantages, i.e. diminished risk of systemic adverse side effects, very rapid and immediate onset of action, high local doses (up to milligrams) can be achieved and the first pass effect can be avoided by bypassing the metabolism inside the liver [3]–[5]. In fact, the pulmonary system with its ample blood stream (5 L/min), large surface area (75 m² - 100 m²) and the extremely thin epithelium (0.1 µm – 0.5 µm) is perfectly tailored to distribute the active pharmaceutical ingredient (API) through the whole body [5], [6]. However, pulmonary administration is a very complex mechanism where several aspects like type of inhaler, DPI formulation and patient's physical condition have to be taken into account [7]. Consequently, it is of utmost importance to understand the structure and function of the human respiratory tract in relation to the interactive powder blend characteristics to achieve the required drug concentration in the targeted lung tissue.

1.1. The respiratory tract

The respiratory tract represents a complex system composed of airways that can be divided in two parts, upper and lower ones (Fig. 1). The former consists of the mouth, the oropharynx, the larynx and the glottis. In its turn the lower part is composed by the trachea, primary bronchi, bronchioles and the alveolar ducts ending up in the alveolar sacs that contain bundles of alveoli surrounded by blood vessels. Between alveoli and blood vessels the unrestricted gas exchange occurs assuring blood oxygenation [7]. The whole respiratory system is an arborescent construct that divides several times (23 times), forming numerous branches [8]. After each bifurcation two new airways emerge, resulting in the duplication of the airways after each branching. As a consequence, the cross sectional area of each subsequent airway decreases, while the cross sectional area of all airways increases after each bifurcation. This leads to a decelerated airflow and change in the flow pattern from turbulent in the trachea to laminar in the alveoli, reducing the airflow resistance inside the airways [9].

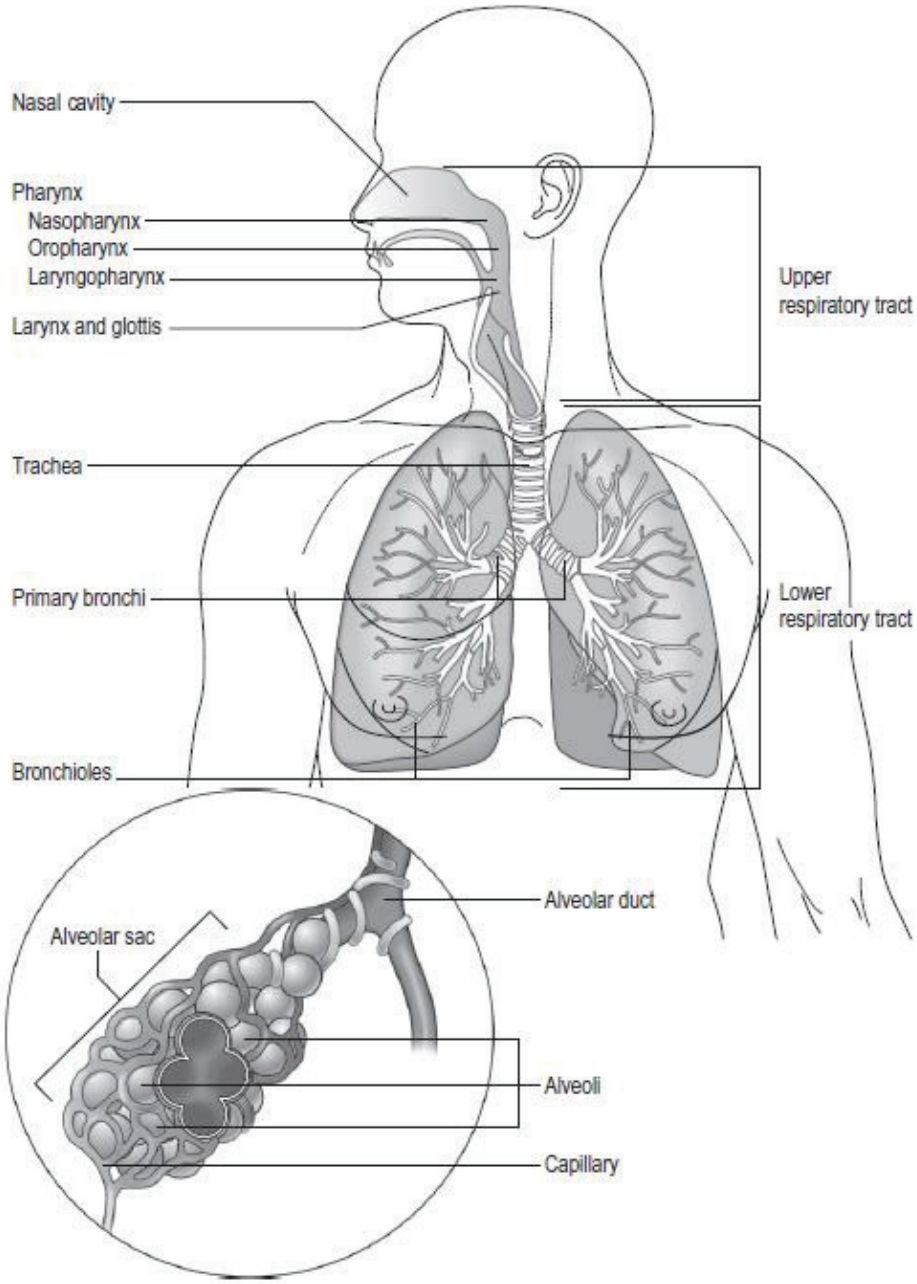

Fig. 1: Illustration of the respiratory tract with its subparts [8]

1.2. Deposition of inhaled particles

The deposition of inhaled particles is determined by several factors, such as the airway geometry, airflow velocity and particle shape. However, API particle size and its distribution is the parameter more often times considered when engineering particles for pulmonary drug delivery [10]. Thus, it is generally accepted that particles have to be in the aerodynamic size range of 1 to 5 µm [11] in order to be able to penetrate into the alveoli and achieve a therapeutic effect. The aerodynamic diameter of an arbitrary particle is defined as the

diameter of a sphere with a density of $\rho = 1$, that settles in still air with the same velocity as the considered particle. It can be expressed with the following equation:

$$d_{AE} = d \cdot \sqrt{\frac{\rho}{\rho_0 \cdot \chi}} \quad (1)$$

where d_{AE} is the aerodynamic diameter, d the diameter of the sphere, ρ is the density of the arbitrary particle, ρ_0 equals unity and χ incorporates the shape of the considered particle [5], [10]. Furthermore, particles designed for inhalation are of different sizes. Therefore, to describe such a particle size distribution, the mass median aerodynamic diameter (MMAD) is often times used. This denotes the diameter of a particle where 50% of the total aerosol mass has a smaller and 50% has a larger particle diameter [3].

The deposition of particles inside the airways can take place by three main mechanisms: inertial impaction, sedimentation due to gravity and Brownian motion (diffusion) [7], [10], [12], [13]. Particles with aerodynamic diameters larger than 5 µm and as small as 2 µm are mostly affected by inertial impaction. Particles that impact by this mechanism are not able to follow the trajectory of the surrounding fluid, depositing most commonly in the upper airways down to the primary bronchi [12], [14], (discussed in more detail in section 1.6.). Sedimentation is the settling of a particle due to the gravitational field and its density difference in relation to the surrounding fluid. It affects aerosols in the size range of 0.5 to 5 µm. Deposition via the former can take place in the upper airways, however it also occurs in the lower ones and thus embodies a necessary part of the therapeutic effect of inhaled powders [12]. Small particles (< 0.5 µm) are mainly deposited due to diffusion. Aerosols in this small size range are strongly exposed to collisions with the surrounding gas molecules and consequently exhibit a random movement (Brownian motion). These particles primarily deposit in the alveoli where the velocity of the air is very small [7].

1.3. Inhalation devices

In regard to the applicability and the efficiency of pulmonary drug delivery the inhalation device represents a very important component. Its design is decisively influenced by the claims of the patients [15]–[17]. Therefore, a good inhaler should combine different properties. It should be user-friendly, portable and it should be possible that patients with differences in their physical performance can use it equally [15]. On the market one can find three different types of devices for the pulmonary drug delivery, (1) pressurized metered-

dose inhalers (pMDIs), (2) nebulizers and (3) dry powder inhalers (DPIs), each of these three having its advantages and drawbacks [5], [18]. Moreover, all of these three types have their own approach to deliver the drug to the lung. They vary in the dosing principle and the used formulation. For instance, pMDIs use formulations where APIs are either dissolved or dispersed in a propellant. During actuation, the formulation gets nebulised and hence inhalable for the patient [17]. Nebulizers also use the principle of nebulisation of a suspension or aqueous solution that contains the API. However, they are usually used as stationary devices and only very seldom as portable ones [15], [16]. DPIs in comparison to the other two devices use dry formulations [15]–[17]. In this thesis the main focus is put on capsule based DPIs, DPI-formulations and their applications, thus these topics will be discussed in more detail in the following chapters.

1.3.1. Dry powder inhalers

Due to drawbacks in dealing with nebulizers and pMDIs a new device came up in the second half of the past century, the dry powder inhaler system. The first dry powder inhaler system was put on the market in the late 1960s. Over the past decades a great deal of effort has been put in the research and the development of this type of formulation and device and is still taking place [19]–[21].

In principle, the common design of all DPIs, is made up of three different parts. Each part contributes to the aerodynamic performance and hence to the efficiency of pulmonary drug delivery, namely (1) the DPI formulation, (2) the dosing/container system and (3) the device with the powder de-agglomeration unit and the mouthpiece [1], [5].

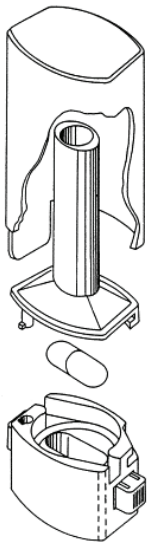

Fig. 2: Schema of a capsule based DPI [22]

DPIs can be divided into different categories. The single dose ones where a capsule or blister is filled with a metered powder that contains the API (Fig. 2) and the multi dose ones where a formulation is stored in a reservoir container and metered upon activation. These two types can be summarised as passive devices or breath-actuated devices, which trigger powder release by the inhalation of the patient. The pulmonary drug delivery with these devices depends on the respirable flow rate achieved by the patient [16], [23], which can lead to complications if patients are not able to breath in deeply [15]. On the other side there are active DPIs, which use integrated facilities like electrically operated impellors to support the powder dispersion [17]. They are very expensive and complicated to operate, thus they are rarely in use [17], [23]. The initial DPIs, which came on the market and which are still in use are the single dose ones. In a single dose DPI system, at first the capsule or blister is pierced by the inhaler device, followed by a deep breath of the patient to release the powder from the capsule or blister and deliver the API particles to the lung. As the name already implies the capsule is designed only for one single application after that the device has to be refilled again with another capsule to be ready for another usage [17]. To overcome the tedious refilling procedure, multi dose DPIs were developed which comprise several drug doses. It can be distinguished between two different formulation storage systems for multi dose DPIs. The powder can either be filled in an attached reservoir from which it is metered into single doses by hand or the DPI device contains blisters filled with single doses that are manually turned to the next blister for administration of the next dose [24]. In comparison to the use of capsule or blister devices a big challenge for reservoir multi dose DPIs is the provision of equal doses for each inhalation, which requires the right metering of the DPI formulation and a sufficient flowability of the formulation [1].

Two different formulation principles are used for DPIs, namely soft spherical pellets and adhesive mixtures [1], [25]. Soft spherical pellets are spheronized agglomerates of small drug particles which are sieved to obtain easy dispersible pellets of sizes between 200 – 2000 µm. Adhesive mixtures are so called carrier based formulations, where the fine API is mixed with a coarser carrier [1], [2], [26]. Nowadays the carrier of choice is lactose monohydrate because it fulfils all safety requirements, it is globally available and relatively cost efficient. However, there are also some minor important carriers available, mannitol, dextrose, xylitol, etc., which are already examined in literature and even partially in use for marketed DPIs [5]. Carrier based formulations present some important advantages in the application of DPIs [26], [27]. In order to reach the lung the API particles within pulmonary formulations have to have an aerodynamic diameter of about 1 – 5 µm, as already mentioned in the section 1.2. [28]. However, these small sized range particles have high tendency to be cohesive, detrimentally impacting formulation’s flowability required for accurate dose

metering. Therefore, to improve flow properties, reduce dosing problems, and providing a high drug content, carrier particles are blended with the API, forming an interactive powder mixture [29]. In this type of mixtures the small API is attached to a coarser excipient due to interparticle interactions [30], which are described in more detail in section 1.4.3. Adhesive mixtures used for DPI applications have to fulfil some specific criteria. The API should be distributed homogeneously over the carrier. A stable mixture, able to provide good processing, storage and transport should be obtained without detrimentally impacting API separation from the carrier surface during inhalation. Because if the API stays attached to the carrier during inhalation it will settle in the oral cavity and no therapeutic effect is achieved [1]. To provide an ideal balance between adhesion during processing and aerosolisation during inhalation, many factors have to be taken into account: carrier payload, mixing conditions, environmental conditions, inhaler design and particles' physicochemical properties [1], [19], [29]. DPI inhalation device design, for example, can have a major influence on the air flux through the device, with specific components of the inhaler influencing particle de-agglomeration and detachment to ensure sufficient drug dispersion [31]. Since most of the dry powder inhalers are breath-actuated devices the forces necessary to detach the drug particle from the carrier surface depends on the respirable flow rate of the patient. Shear, inertial, drag, friction and lift forces are thereby engendered, whereas inertial forces are the most critical ones to overcome drug-carrier adhesive forces. Inertial forces arise due to particles that collide against each other and with the device walls, being that these are the only forces able to cause detachment of drug particles adhered tightly to the carrier. The magnitude of the inertial forces increases with the third power of the diameter of the considered particle. Drug-carrier separation is generally enhanced when the air flux through the inhaler is increased [1], [32]. Thus, to achieve a good inhalation effect, it is important to inhale sufficiently strong and over a considerable time [33]. In regards to particles' physicochemical properties and abundance of research has been done in an attempt to understand which particle properties can critically impact API-carrier interaction [20], [34]; with engineering of these properties being widely tried in order to improve DPI efficiency, however downstream processes' impact (e.g. mixing) on formulation characteristics has been often times overlooked and rarely considered in available literature [20].

1.4. DPI formulation

The DPI formulations of interest for this thesis and which were used in the experimental part were carrier based. Producing adhesive mixtures for DPIs requires API particles in the inhalable size range (see section 1.2.) to reach the small airways of the deep lung in order to

achieve a therapeutic effect. Such small drug particles are usually not available from crystallization and have to be processed or engineered.

1.4.1. Particle engineering

In the literature several methods are described to reduce the particle sizes of APIs, like jet milling [35], spray drying [36] and several other techniques [15], [30]. Each of them produces particles with unique physicochemical characteristics that can further affect processing and inhalation performance [1].

Milling is a frequently used unit operation to reduce drug particle sizes, with jet milling being the preferred one to produce particles in the aerodynamic size range. Gases, usually air, injected at high pressures are used to fluidise the raw powder that is continuously introduced in a milling chamber. Consequently, particle collisions arise, causing the micronization of particles down to 1 µm. With this technique it is quite challenging to engineer particles with controlled physicochemical properties. Jet milled particles are predominantly irregular, elongated needle like crystals [5].

By contrast, the spray drying process is better controllable, producing particles with uniform shapes and morphology, thus it is frequently used in the production of drug particles for pulmonary delivery. The fundamental principle of this technique is the precipitation of solid particles out of an emulsion, solution or suspension. The raw material is atomised into small droplets, which are exposed to a co-current hot gas stream, causing the evaporation of the liquid and the subsequent precipitation of the dried particles that are finally separated, out of the gas stream, commonly with a cyclone [37]. The first two steps of spray drying, atomisation and drying, both strongly affect the final physicochemical properties of the drug particles. As a consequence, it is important to use the right atomisation technique, drying temperatures, residence time, flow rate of the gas, etc., to obtain particles suitable for pulmonary drug delivery. However, this also offers a great opportunity to engineer drug particles with one's defined and desired physicochemical properties [38]. In theory spray dried particles are spherically shaped and should exhibit a narrower size distribution compared to micronized particles [5]. Concerning solid state, spray-dried particles usually solidify in the amorphous phase [37].

1.4.2. Particle properties

The physicochemical properties of both involved particle parts, carrier and drug, may have strong impact on further processing (blending, capsule filling, etc.) and finally on the aerodynamic performance of the formulation. Consequently, in order to be able to produce potent adhesive mixtures it is necessary to analyse and understand the influence of particle properties, since they predominately affect cohesive and adhesive interactions. Whereas, adhesive forces acting between particles with different properties and cohesive forces among particles with similar properties [39]. These properties include the solid-state of the material, particle size, size distribution and shape and surface morphology [38].

As mentioned in 1.5.1., different engineering techniques are able to produce API particles with different solid structures. In amorphous structures contrary to crystalline ones, atoms are randomly positioned in relation to each other, lacking in long range order and thermodynamic stability. Compared to long range ordered materials (crystals) due to their disordered state amorphous materials present higher internal and surface free energies and molecular motions. This in turn can lead to increased interparticle cohesiveness and adhesiveness detrimentally affecting DPI product performance [40].

The particle size is often the most crucial property in the design of solid dosage forms. Regarding DPI formulations the drug particle size is of utmost importance in order to guarantee that drug particles are able to penetrate into the small airways. Furthermore, particle size strongly influences the forces acting on a particle. Kulvanich et. al. (1987) showed that adhesion forces increase with decreasing particle size [41]. In the size range below <10 µm adhesion forces exceed gravitational ones and particles in this size range become able to adhere to larger ones. So, naturally size becomes a basic requirement when producing adhesive mixtures. In another study drug particle size was related to particle detachment during inhalation [42]. It was observed that increasing the drug particle size enhance particle aerosolisation. Consequently, it is essential to determine the powder particle size distribution. Since particles of a powder are usually heterodisperse, i.e. different particle sizes are present, the particle size distribution (PSD) is measured. The PSD of a powder is presented with different distribution function (e.g. Gaussian distribution, log-normal distribution), which can then be used to determine a mean particle size, e.g. mass median aerodynamic diameter (section 1.2.). Also particle shape has to be considered when developing a DPI formulation. Shape is a predominant factor for the interparticle forces, being widely accepted that higher contact areas and shorter interparticle distances, lead to stronger adhesion forces [40]. So when compared to spherical ones (e.g. produced with

spray drying), irregular shaped drug particles (e.g. flat or needle shaped, produced with jet milling) are expected to be more cohesive/adhesive. Moreover, particle shape also has a great impact on the flow behaviour of dispersed particles; with elongated, needle like particles being very aerodynamic [43], resulting in smaller aerodynamic diameters compared to spherical ones. Thus, when compared to spherical drug particles of equal mass, elongated ones will be better dispersed in a gas stream and penetrate further within a branching system (e.g. the lung) [40].

Finally it is important to address the particles' surface morphology, since it represents the interface of adhesion and cohesion between the involved particles. The morphology of the particle surface primarily determines the contact area between drug and carrier particles and thus the magnitude of adhesion forces [40]. Regarding the carrier surface one central concept has to be taken into consideration. Carrier surface is formed by the so called 'active sites'; these are spots where fine drug particles primarily and strongly adhere to. These 'active sites' are caused by several reasons, i.e. impurities, surface asperities, crystal lattice defects, etc. [30]. Therefore, understanding and controlling the surface morphology is essential in the design of DPI formulations.

In regards to drug particles, different engineering techniques result in different solid structures with different surface morphologies (section 1.4.1.) which consequently influence particle interaction. For instance, molecular disordered spots, exhibiting enhanced surface energies can be randomly induced on the surface of the jet milled particles, leading to increased particle cohesiveness and adhesiveness [44]. The surface energy of a material can be described as the energy needed to increase the surface area of a solid particle. To add to the former, particles with different morphologies will also exhibit different surface energies [40]. It is generally accepted that drug particles with high surface energies adhere more tightly to the carrier surface [45]. Furthermore, difference in solid surface structures influence the water uptake of the particles. Amorphous surface structures tend to adsorb large quantities of water, potentially leading to alteration of the particle's morphology. Surface characteristics can also significantly impact triboelectrostatic charging of particles, a phenomenon very likely to occur during powder blending. Through particle collisions surfaces come into contact and rub against each other leading to electron transfer once the two surface separate. For example, round, smooth, amorphous particle surfaces (e.g. produced with spray drying) lead to a relatively fast and homogeneous distribution of the induced charges through particle surface, leading to a faster dissipation of former. In contrast in more edged crystalline particles charges can accumulate in the sharp corners, resulting in an inconsistent charge distribution [40] and longer charge retention. Since electrostatic forces

are important in particle interaction, especially for small particles, this phenomena has to been taken into account when producing adhesive mixtures for DPIs.

Formulating adhesive mixtures not only demands the understanding of the morphology of the drug particle, but also that one of the carrier. As explained above, the 'active sites' on carriers' surface can be due to numerous characteristics, however surface morphology, in particular rugosity vs smoothness, are very important parameters to take into consideration when studying carrier-drug interactions. Rough carrier surfaces exhibit clefts and cavities where drug particles can preferably adhere and accumulate during mixing. Drug particles in these cavities compared to that ones on the plane surfaces of the carrier are not influenced by the press on forces, namely the inertial and frictional forces which arise during mixing, due to particle-particle and particle-wall collisions. As a consequence, the rougher the carrier surface the more space is available for particles to be sheltered from press on forces appear, which subsequently can affect particle detachment during inhalation [46]. This also has to be taken into consideration when altering the carrier payload, namely the amount of drug particles attached to the carrier surface. The higher the carrier payload the less drug particles are able to adhere to the preferred asperities. This results in a weaker drug-carrier interaction which can, possibly, lead to a better drug release during inhalation. [30]. However, it was also reviewed that this could have an adverse effect on the aerosolisation performance [20].

In conclusion, regarding mixing and in particular adhesive mixing, it is essential to take the physicochemical properties of the different interacting particles into consideration in order to provide potent DPI formulations.

1.4.3. Powder mixing

The blending of different powders is a crucial unit operation in the production of suitable formulations for DPIs, as well as in the whole pharmaceutical industry. The primary objective is to obtain powder blends that exhibit a high mixing homogeneity and which show low tendency to segregate. The first investigations into blending of different powders described mixing as a complete randomised process, where a permanent disorder is introduced into a particle arrangement and a disorder maximum is achieved, when an equilibrium state is reached. Thus, this disorder maximum can be represented as the highest possible degree of mixing homogeneity of a powder blend, where ongoing mixing would always lead to equivalent results of mixing homogeneity [47]. This theory of random mixtures is limited to the blending of particles within similar size ranges and without cohesive forces acting among them. Taking this shortcomings into account, Hersey (1975) further developed this concept

[48] and the term ‘ordered mixture’ was created. The former describes a mixture with a high degree of homogeneity where small particles are able to adhere to the surface of larger ones. Staniforth (1981) adjusted this theory and introduced the term adhesive mixtures, which is still valid today [49]. In these mixtures both adhesion and cohesion are present among the particles, whereas it is unpredictable which one predominates, since it strongly depends on particle properties [50].

Adhesive mixing, as mentioned in section 1.3.1., is the preferred formulation strategy for DPI products. The engineered inhalable drug particles are mixed with larger carrier ones (with a size of around 100 µm) because of the two following main reasons; (1) with the addition of the carrier, the flow properties of the formulation are enhanced and dosing can be achieved more easily and precisely [2] and (2) as the small drug particles attach to the surface of the coarser carrier ones, detrimental effects on downstream processing, such as segregation, are minimized. The interactions between the drug and the carrier are mainly driven by the interplay of van der Waals (VdW), electrostatic and capillary forces [30]. VdW forces are the predominate ones and arise due to inconsistent distribution of electrons inside an uncharged molecule, resulting in temporary dipoles. Whereas, electrostatic forces act between charged particles and capillary forces appear when a liquid film forms between the surfaces of two particles [40].

Adhesive mixing is a fundamental process in DPI development, so when formulating these type of products it is important that one understands the series of concepts behind powder mixing. The complete powder mixing process is very complex and it depends on several factors, like mixing conditions (mixing time, rotational speed), mixer type, properties of the drug and carrier, etc. [20]. Mixing of dry powders always requires an agitation of the powder bed, leading to an ongoing spatial position change of the particles until the equilibrium state is reached. This can be accomplished by two different mechanisms which vary significantly in the level of the energy input. Powder mixing can either be achieved with a rotating container that causes a cascading movement of the powder bed (tumbling blenders / low shear blenders) or with an implemented rotating impeller which churn the powder bed thoroughly (high shear blenders). Convection, diffusion and shearing are critical for the mixing performance. Shear stresses are very important for adhesive mixing because they are the ones partially responsible to break up the drug particle clusters and thus providing an evenly distribution over the carrier [30], [51]. Manufacturing of adhesive mixtures can be divided into a sequence of four different steps where the individual steps can sometimes intersect (Fig. 3). At the beginning, the carrier particles and the smaller drug agglomerates are randomly mixed, followed by the break-up of the drug-drug particle interaction due to shear forces

which arise during mixing. The lose drug particles then adhere to the carrier surface and get continuously redistributed over the carrier's surface due to frictional and inertial forces [52], [53].

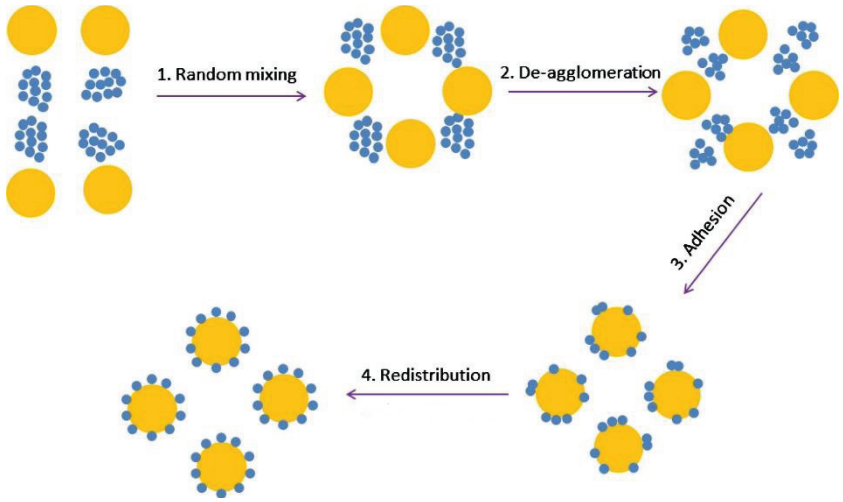

Fig. 3: Mixing steps in the production of adhesive mixtures [53]

As mentioned in section 1.3.1. the main objective of adhesive mixing is to obtain homogeneous and stable blends that additionally show good detachment properties of the drug particles during inhalation. Meaning that the API should be distributed very consistently and tightly enough over the carrier particles' surfaces so that it does not detach from it during processing (but only during inhalation). Thus, a prerequisite for a successful DPI adhesive mixture is that the drug-carrier interaction has to be stronger than the drug-drug interaction. These interactions are mainly impacted by the frictional, shear and inertial forces that occur during mixing [20] and which are mainly depend on the type of mixer used.

As the focus of this thesis is put on the mixing performance using a tumbling blender it is important to mention that available literature shows that duration of the mixing and rotational speed are key parameters when working with this type of blenders. The mixing time has a strong influence on the drug-carrier interaction [11], hence longer mixing increases the period during which press on forces can act on the particles. Concerning rotational speed it is known that shear forces are increased when the former is enhanced, leading to a more efficient break up of drug clusters [54]. Both strategies result in more homogeneous blends. However, there is an upper limit for both parameters where a further increasing would not result in better mixing homogeneities. Since at specific settings mixing and de-mixing are in equilibrium. Therefore, it is important to find out the briefest mixing time and the lowest rotational speed able to obtain a powder blend with acceptable mixing homogeneity and which furthermore shows adequate drug detachment during inhalation [20]. A tolerable

mixing homogeneity defined by the FDA has to display a relative standard deviation (RSD) of the API content below 5% [55], [56].

1.4.4. Powder bulk

The appearance and behaviour of the powder bulk is dependent on several factors. This includes the particle properties mentioned in section 1.4.2. It was for example reviewed that spherical-shaped particles exhibit a higher flowability compared to more irregular-shaped ones, due to less interparticle contact points [20], [57]. Furthermore, different blending methods, inducing various magnitudes of forces and stresses on the particles also affecting the powder bulk. Leading to more or less cohesive powder mixtures with different flow behaviours, which subsequently promote or reduce the aerodynamic performance [20]. Therefore, it is important to investigate the behaviour of a powder to be able to draw conclusion concerning the powder performance during mixing, dosing and aerosolisation. The analysis of a powder in motion, i.e. ‘dynamic powder characterisation’ [58], is often used to determine different parameters which affect powder rheology. A sophisticated equipment for such measurements is a so called Powder Rheometer, like the FT4 (Freeman Technology, Tewkesbury, United Kingdom). It contains elaborated measurement methods (shear cell, permeability, etc.) that allow to investigate how powders aerosolise, react on induced forces, compact or transmit fluids, which all must be considered in the production of DPI formulations. A disadvantage, however, of this apparatus is that the comparison of different measurement results is often challenging [59]. The individual methods and measured parameters describing the powder rheology are discussed later on in section 3.3.

In principle, the powder bulk properties of adhesive mixtures for DPIs usually depend on the carrier. It is widely approved that poor carrier flowability and low carrier bulk density adversely affect mixing homogeneity and facilitate segregation [20]. The properties of the carrier bulk have also strong impact on the press on forces during powder blending [11]. However, if the carrier payload gets higher the drug particles can also critically influence the bulk of an adhesive mixture. High drug to carrier ratios may result in a multilayer formation of adherent drug particles, even already before the carrier surface is covered with a complete monolayer [41]. Furthermore, it can lead to a complete saturation of the carrier surface, meaning that loose not attached drug particles remain. Resulting in the agglomeration of the latter, segregation and subsequently worse mixing homogeneity [60]. Therefore, it is advisable to adjust the carrier payload to the physio-chemical properties of the carrier [20], to guarantee that all drug particles are able to adhere to the carrier surface.

1.5. Capsule filling of dry powders

Capsules filled with the DPI formulation are commonly used as a metered dose container for single doses for DPIs. In DPIs the formulation consists either of an API or an API blended with a larger carrier, and the typical amount of the total inhalable powder is less than 40 mg. As APIs become more potent, there is a trend towards lower-fill-weight systems. This requires a very accurate low-dose capsule filling process. In the past, two-piece hard capsules made out of gelatine have been used. Nowadays more and more capsules based on hydroxypropyl methylcellulose (HPMC) are applied for DPIs because they have some beneficial attributes. They usually do not react with the filling material, they allow good discharge of the formulation and they are less sensitive to low humidity conditions. [61].

There are several equipment, with different filling mechanisms, available to fill dry powders into hard capsules. In general, the capsule filling machines can be categorized in manually, semi-automatic and fully automated ones. Furthermore, they can be classified due to their filling principle in direct or indirect filling machines. In the direct filling principle the metering occurs directly into the capsules. In indirect filling methods the needed dose is first drawn by an implemented dosing unit and afterwards transferred into the capsule. A mechanism that belongs to the first category is the auger filling mechanism. It uses a hopper with a built in auger which is filled with powder. The capsules are placed on a rotating plate at the outlet of the hopper. Due to the motion of the auger, the capsules get filled with powder. Another direct filling technique is the filling caused by vibration. The DPI formulation is filled in a container with an oscillating sieve at the bottom, thus the powder percolates through into the capsules which are aligned below the container. The second class contains the tamping principle which uses usually six tamping pins, which sequentially compress little amounts of a powder bed into dosing bores to form a powder plug, which is then released into the capsule at the sixth step. Moreover, the vacuum drum filling principle, which applies vacuum to take up powder into the cavity of a dosator and afterwards release it again into the capsule, and the dosator system belong also to the indirect filling category [62] and are preferentially used for low-dose capsule filling. The latter will be described in more detail in the following chapter, because it is the filling principle, which is used in the experimental part of this thesis.

1.5.1. Dosator filling principle

Dosator filling machines usually work fully automated and they are available from lab scale up to industrial scale, the latter are able to eject a few hundred thousand capsules per hour. They can handle all capsule sizes and fill different amounts of doses [61]. The basic set-up of

a dosator filling machine contains a hopper via that the powder (e.g. DPI formulation) is continuously fed into a rotating container. Inside the rotating container fixed scrapers form a powder bed with a defined height (Fig. 5). For metering a dosator dips into the powder bed (compacts it) and collects the desired volume of powder from the powder layer into a dosing tube. After collecting the powder, the dosator is lifted up again, rotates further and stops beyond a gap. Under this gap a chain with opened capsules is pulled through in which the gathered dose is discharged (Fig. 4).

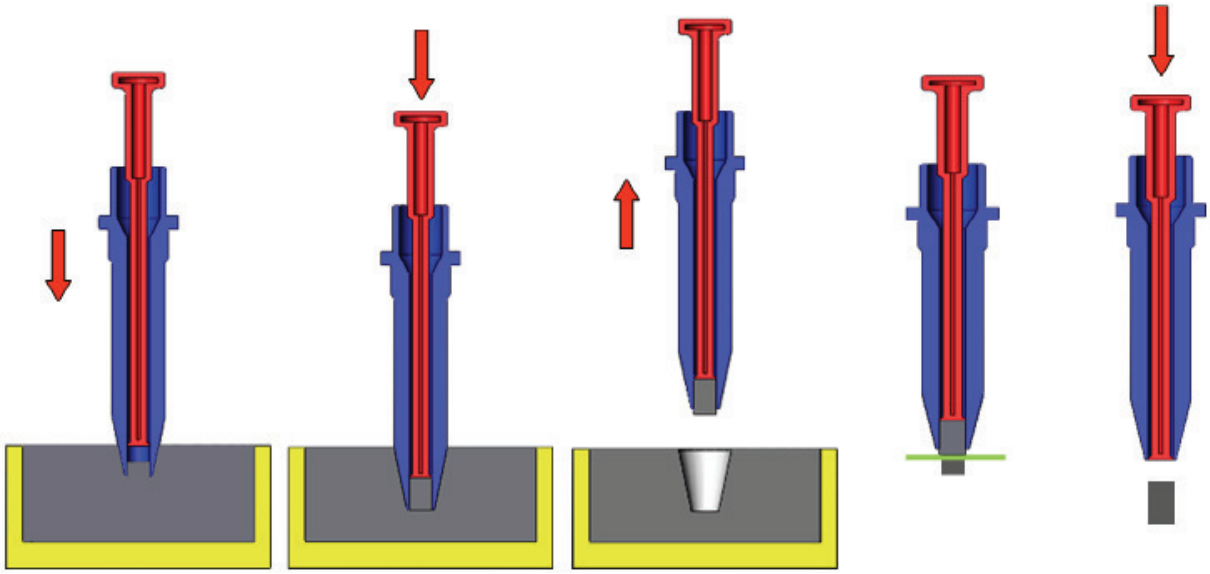

Fig. 4: Individual steps of the dosator filling principle [63]

The dosator itself comprises several components, the main part is the dosing tube. Inside the tube a moveable piston is mounted, which is responsible for the powder discharge. The piston is able to move up and down due to the compression and relaxation of an integrated spring and thus allowing the discharging of the powder out of the dosing tube (Fig. 5) [62]. Thereby it becomes also possible to additionally compress the powder bulk via the piston to form a stable powder plug. However, this feature is not used for DPI capsule filling, since firstly dosing is still accurate and secondly highly compacted powders would adversely affect aerosolisation of the API particles [64]. The amount of the dose can be varied as different dosing chamber lengths (bordered by a moveable piston) and different dosator diameters can be used, resulting in different cylindrical volumes (dosing chambers). Additionally the powder bed height can be varied to increase the compression of the powder [61].

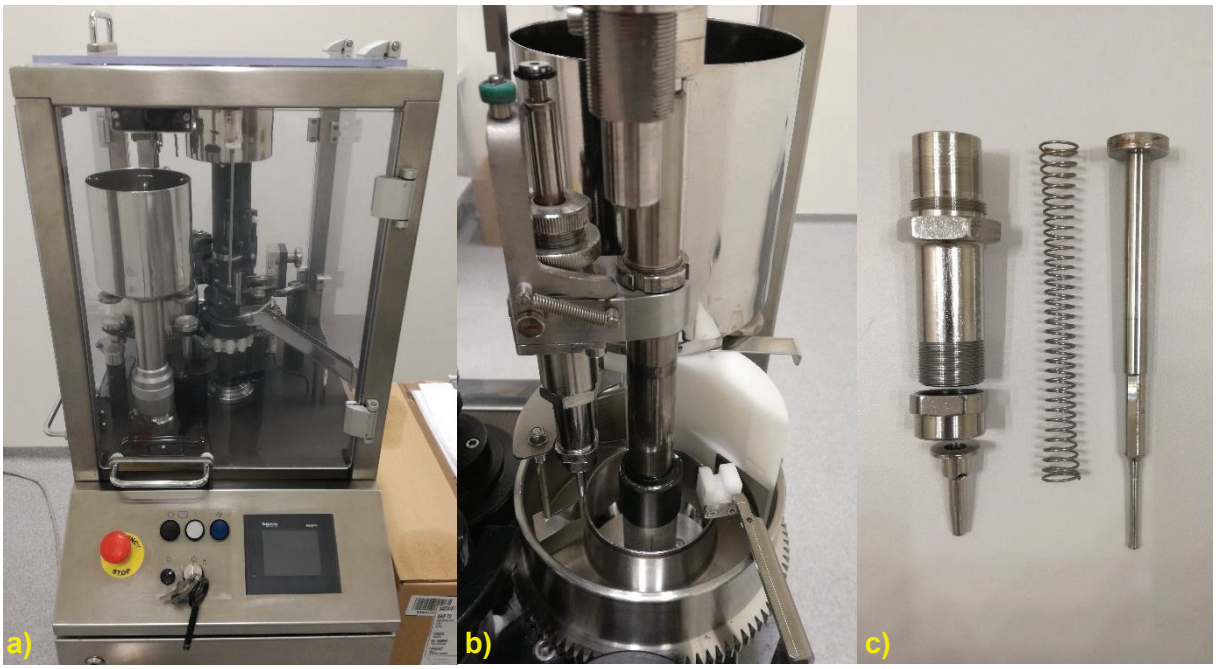

Fig. 5: a) Labby capsule filling machine b) Assembled capsule filling unit (with dosator, rotating container and scrapers) c) dosator parts in detail

An adequate capsule filling process depends on several particle and bulk properties, like particle size, shape or the cohesion of the powder. In general, a prerequisite for the dosator system is arching of the powder inside the dosing tube otherwise filling with this method is completely impossible. Therefore, frictional forces between the powder bulk and the dosator tube wall have to exceed the gravitational forces in order that the powder remains in the dosator and does not drop out. That can be regulated by changing bulk properties and/or the diameter of the dosator opening. A very crucial factor for capsule filling is the flowability. Regarding dosator capsule filling a compromise has to be made. Excellent flow properties of the powder yield a consistent powder bed and uniform dosing, however, the powder is then nearly incapable to form an arch inside the dosator. On the other side, poor flowability exhibits exactly the reverse phenomena. Consequently, the perfect powder flowability has to be somewhere in between to support arching and uniform dose metering. Thus, it is important to characterise the flow properties to draw conclusions about capsule filling [59].

1.6. In vitro performance of DPI formulations

When developing a new DPI formulation it is important to test its in vitro aerosolisation performance to have insights into its possible in vivo action. For this reason and in order to simulate the aerosol deposition inside the human lung, impingers, impactors and standardised procedures for testing using the former can be found in official documents, such as the U.S. Pharmacopoeia [65]. The main set up difference between the impingers

and impactors is the medium in which particles deposit. For instance, impingers use liquid impaction plates, whereas the impaction plates in impactors are dry. Excluding the former, a similar set-up can be found in both of these devices; a mouthpiece fixed on a 90° angled inlet tube, followed by a series of impactor plates with a filter at the end where non-deposited particles are collected. An airstream through the apparatus is applied using a vacuum pump. Typical apparatuses are the twin stage impinger, the multi stage liquid impinger and the two cascade impactors, the Anderson cascade impactor and the next generation impactor (NGI) [33].

Today's favoured impactor is the NGI. This has a horizontal setup comprised of three main parts, the cup tray, the frame that holds the cup tray and the cover with the fixed nozzles and the inter-stage pathways (Fig. 6 and 7). The NGI contains seven impaction stages and additionally a micro-orifice collector that acts as a filter and is responsible for collecting the finest fraction. The air enters the impactor through a bended inlet tube that is adapted into a pre-separator, where the coarse carrier particles are collected. Inside the NGI the air streams zig zags from stage to stage, through nozzle diameters that decrease stepwise. Consequently, air velocity increases, leading to a decreasing particle cut off diameter as impactor stages progress from one to seven (plus filter) [66]. So, each stage has a specific cut off size that can be calibrated, consistently. Since the airflow rate can be varied in the range of 28 l/min to 100 l/min when assessing a DPI, the cut off diameters of the individual stages change as well. Although it is possible to calculate the cut off sizes for all flow rates if the cut off size for a specific flow rate is known, the following relationship is valid:

$$d_{50,Q} = d_{50,Q_n} \cdot \left(\frac{Q_n}{Q}\right)^x \quad (2)$$

where d_{50,Q_n} is the cut off diameter of the standardised flow rate Q_n (often 60 l/min) and $d_{50,Q}$ is the cut off of the applied flow rate Q. The variable x depends on the individual stage and varies from 0.54 at stage 1 to 0.67 at stage 7. This implements the higher the flow rate the smaller the cut off diameters for the individual stages [33]. To provide an adequate correlation between the in vitro assessment and the in vivo action of the DPI, a fixed air volume of 4 l per test should be sucked through the device, since this is the volume that an average adult is able to inhale [33].

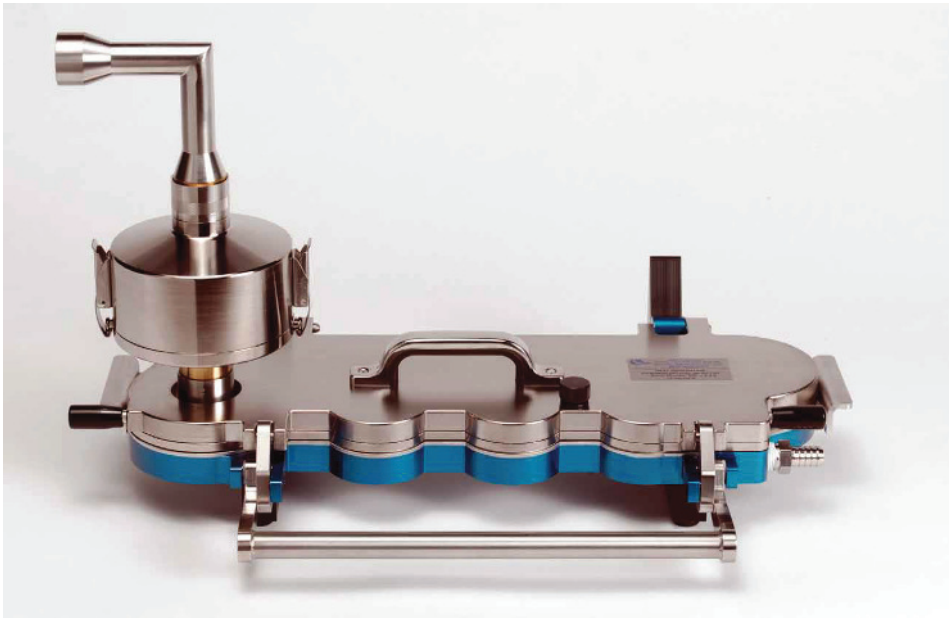

Fig. 6: Closed setup of the NGI with the 90° bended inlet tube and the pre-separator [66]

Fig. 7: Open NGI with the cup trays and the injector nozzles on the cover [66]

DPI formulation in vitro assessment is based on inertial impaction of aerosols [33]. Particles get fractionated according to their various sizes and from this it is possible to determine the particles' aerodynamic diameters (section 1.2.). It is known that aerosols present particles of different sizes that exhibit different amount of momenta, the product of the particle mass and its velocity. For instance, particles with large aerodynamic diameters and thus heavier ones have a high momentum, not able to adjust fast enough when the air stream changes direction and impacting earlier than small particles that are transported further. Thus, the impaction probability of aerosols can be calculated with the Stokes' number of a particle (Equ. (3)), being that if it exceeds unity particles tend to impact.

$$Stk = \frac{\rho_p \cdot d_p^2 \cdot u}{18 \cdot \mu \cdot d} \quad (3)$$

The parameters ρ_p and d_p are the density and the diameter of the considered particle, u is the velocity of the fluid, μ is the dynamic viscosity of fluid and d is a characteristic diameter, e.g. of the specific airway [12]. So based on the former during in vitro testing aerosols will impact and deposit on the different NGI stages according to their size [33]. The mass of impacted particles per stage can then be used to investigate the aerodynamic performance of a DPI-formulation and characteristic parameters such as fine particle dose (FPD), emitted dose (ED) and fine particle fraction (FPF) can be determined. The fine particle dose is the mass of particles with an aerodynamic diameter smaller 5 µm. When the FPD is related to the total amount of drug deposited in the impactor, the emitted dose (ED), one can determine the percentage of particles able to achieve a therapeutic effect, the fine particle fraction [65]–[67].

1.7. Aim of the thesis

The majority of marketed DPI products consist of binary mixtures of very low doses of API at very low drug loads (generally around 1 - 2%) with the carrier. However, the development of new drug entities (such for e.g. protein like substances) needed to be delivered in higher doses to or through the lung has changed the DPI formulation landscape. This shift from low to high API doses, poses many challenges, in particular the production of stable adhesive mixtures with adequate flowability and good aerodynamic behaviour. Thus, a step-wise, science based approach able to pinpoint the influencing parameter [35], critically impacting mixing, flowability and aerosolisation behaviour of new DPI products is of the utmost importance. Consequently, the aim of this thesis was to investigate the influence of two different API engineering techniques, jet milling (JM) and spray drying (SD), on the adhesive mixing, capsule filling and in vitro aerosolisation processes when used at drug loads of 1% and 10% of engineered API. For this salbutamol sulphate (SS), a β_2-agonist, and Lactohale 100 (LH100) were chosen as a model API and carrier particles, respectively. Firstly, a suitable mixing strategy, able to guarantee a high strength homogeneous DPI formulation, was developed. Here the mixing time, the rotational speed and the API content were screened and varied within a pre-defined range. Furthermore, also the filling ration during mixing and sieving of the SS before it, were taken into consideration. After the identification of the crucial settings needed to obtain a homogeneous mixture at small scale, the blend was scaled up and the two engineered forms of SS were blended with LH100 at low (1%), as control, and at high (10%) API loads. Subsequently, the flow properties of the blends were

examined and capsule filling was performed. For this, a lab scale low dose dosator capsule filling machine (Labby, MG2, Bologna, Italy) and hydroxypropyl-methylcellulose capsule were used. Finally, the aerodynamic performance of the adhesive mixtures was investigated using a Next Generation Impactor (Copley Scientific, Nottingham, United Kingdom).

2. Materials and Methods

2.1. Materials

The carrier used was α-lactose monohydrate (Lactohale 100, pharmaceutical grade confirm), received from DFE Pharma (Goch, Germany). The raw model API, crystalline salbutamol sulphate in USP 25 quality, was supplied by Selectchemie AG (Zurich, Switzerland). Ethanol absolute, Tween 20 and acetic acid were bought from Sigma-Aldrich (Munich, Germany). The size 3 Vcaps® Plus HPMC capsules were donated by Capsugel (Bornem, Belgium). As a test inhaler, the Aerolizer® (Novartis, Basel, Switzerland) was used.

2.2. API engineering

The provided raw SS particles were engineered to inhalable sizes using the two techniques described below.

2.2.1. Jet milling

Jet milling was executed with a 50 AS spiral jet mill (Hosokawa Alpine, Augsburg, Germany). The injection pressure was 7 bar and the milling pressure was 5 bar. The raw SS powder was manually fed into the hopper. Approximately 40 g of raw SS were milled in each round.

2.2.2. Spray drying

The raw SS was dissolved in purified water (Micro pure, TKA Wasseraufbereitungssysteme GmbH, Niederelbert, Germany), the SS concentration was 7.5 w%. The Spray Dryer 4M8-TriX (ProCepT, Zelzate, Belgium) with a bi-fluid nozzle (Ø 0.2 mm) in open loop configuration was used. The air flow rate through the nozzle was 8.34 ± 0.10 l/min (1.99 ± 0.01 bar). The pump capacity was set to 20%, resulting in a feed rate of 3 g/min. The inlet and outlet temperature of the drying air was 120.04 ± 0.09 °C and 40.92 ± 0.51 °C, respectively. The air flow rate through the drying chamber was set to 0.30 ± 0.01 m^3/min and the pressure drop in the cyclone was 60.49 ± 3.13 mbar.

2.3. Particle and powder characterisation

The particle size, shape and solid state of the LH100 and of the engineered forms of SS were determined. Additionally, the flow properties of the powder blends (adhesive mixtures) were examined (section 2.5.).

2.3.1. Small and wide angle X-ray scattering (SWAXS)

SWAXS measurements were performed to analyse the solid state of the used powders, for both the LH100 as well as for the engineered forms of SS. The characterisation was done with the Hecus X-ray system S3-MICRO (Bruker AXS, Karlsruhe; Germany). The angular range of the WAXS measurement was held between 17° and 28°. For the measurement the samples were kept in rotating capillaries with a diameter of 2 mm, the exposure duration was set to 600 seconds.

2.3.2. Particle size measurement

Laser diffraction technique (Helos/KR, Sympatec GmbH, Clausthal-Zellerfeld, Germany) was applied for particle size characterisation. The powder was fed via a vibrating chute (Vibri, Sympatec GmbH) and subsequently dispersed with the Rodos/L dry dispersion unit (Sympatec GmbH) at a primary pressure of 0.5 and 0.1 bar, respectively. The 4 mm injector and two different measuring ranges R2 (0.45-87.5 µm) and R5 (4.5-875 µm) were used. For the data evaluation the software Windox 5 (Sympatec GmbH) was used.

2.3.3. Scanning electron microscopy

On the one hand scanning electron microscopy (SEM) was used to determine the shape and morphology of the carrier and the engineered API particles, and on the other hand to investigate how homogeneously the API was distributed over the carrier surface in the produced adhesive mixtures. The scanning electron microscope (Zeiss Ultra 55, Zeiss, Oberkochen, Germany) was operated at 5 kV.

2.4. Powder blending

The powder blending can be divided into two different parts. The first one was the screening of the best mixing parameters to obtain powder blends with an adequate mixing homogeneity. This was specified by the relative standard deviation (RSD) of the SS content in the blends; the maximum value was defined to be 5% (see section 1.4.3.). Afterwards the previously screened mixing parameters were applied to up-scaled blends which were subsequently used for capsule filling and for the assessment of the aerodynamic performance.

2.4.1. Screening of the mixing parameters

The screening was performed with the JM SS. 10 g blends with a low and a high API load (1% w/w and 10% w/w) were prepared using the sandwich method. More precisely, a layer of carrier was first put in the vessel, followed by a layer of API and on top of it another layer of carrier. The blends were mixed in polypropylene vessels (filling ratio was approximately 50%) with the low shear Turbula T2F blender (Willy A. Bachofen Maschinenfabrik, Muttenz, Switzerland). Five different mixing conditions (mixing time and speed) were tested (Tab. 1).

Tab. 1: Specification of the mixing conditions

Mixing condition	MC 1	MC 2	MC 3	MC 4	MC 5
Mixing time [min]	5	90	5	90	47.5
Mixing speed [rpm]	22.7	22.7	90	90	55

Additionally, it was examined how sieving of the SS before blending and a reduced vessel filling ratio (RFR, approximately 25%) affect powder blending. Brone et. al. have already investigated that lower filling volumes enhance the mixing rate, since more particles are simultaneously in motion [68]. Whereas, the aim of sieving was to break up the API agglomerates to ensure a homogenous distribution of individual API particles within the powder bulk. Sieving was done by hand, using a sieve with a mesh size of 355 µm. To analyse the mixing homogeneity of the produced blends, 5 samples (of approximately 25 mg) were taken with a spatula, respectively. Two samples were sampled from the top, one from the middle and two from the bottom of the powder bulks and afterwards dissolved in buffer (purified H_2O + acetic acid, adjusted to pH = 3). The SS content was measured by high performance liquid chromatography (HPLC) as described in detail in section 2.8. HPLC method.

2.4.2. Blending of the up-scaled blends

The up scaling was done with the blends listed in Tab. 2. The batch size was 370 g, respectively. This was the amount of powder required for capsule filling and the FT4 powder rheometry measurements. The powders were filled in layers into the blending vessel. Blend 1 & 3 were made up of three carrier layers with two API layers in between and blend 2 & 4 were made up of four carrier layers with three API layers in between. The idea behind this extended sandwich method was to provide a good allocation of the SS within the powder bulk already before mixing was even started. The different number of API layers was only due to the different API loads in the blends.

Tab. 2: Specification of the four blends

Blend 1	Lactohale 100 + 1% w/w jet milled salbutamol sulphate
Blend 2	Lactohale 100 + 10% w/w jet milled salbutamol sulphate
Blend 3	Lactohale 100 + 1% w/w spray dried salbutamol sulphate
Blend 4	Lactohale 100 + 10% w/w spray dried salbutamol sulphate

The mixing time and speed of the Turbula T2C blender were chosen based on the screening results, where the combination of a mixing time of 47.5 min and a mixing speed of 55 rpm yielded the most homogeneous blends. Furthermore, the SS (JM and SD) was sieved before blending and for the high API load blends, a RFR was applied (description why these mixing parameters were chosen see section 3.2.1.). The mixing homogeneity was again analysed using HPLC. Therefore, ten samples (approximately 25 mg), three from the top, four from the middle and three from the bottom of the blend were taken and subsequently dissolved in buffer (purified H_2O + acetic acid, adjusted to pH = 3).

2.5. Powder bulk characterisation of the blends

To investigate the relevant powder bulk properties of the adhesive mixtures for inhalation application, different measuring methods (shear cell testing, aeration and permeability) were performed with a FT4 powder rheometer (Freeman Technology, Tewkesbury, United Kingdom). As a reference, the same was done for the pure LH100. The descriptions of the measuring methods are explained elsewhere [69]. For the shear cell method, the 1 ml shear cell module was used and the consolidation stress was set to 3 kPa, imitating the conditions during capsule filling. Cohesion, flow function coefficient (FFC) and angle of internal friction (AIF) were measured. Aeration, the ability of a powder bulk to become fluidised, and air permeability, the ability of a powder bulk to transmit air, were tested with the 25 mm

accessories kit and the external air conditioning unit. The basic flowability energy (BFE), aerated energy (AE) and aeration ratio (AR) were investigated at an airflow velocity from 2 mm/s up to 10 mm/s. For the permeability test, the powder bulk was constrained in the range of 1 – 15 kPa and the resulting pressure drop across the powder bulk was determined.

2.6. Capsule filling process

Prior to capsule filling, the empty HPMC capsules were consecutively numbered and weighed with a Denver SI-234A scale (reproducibility 0.1 mg), as described by Faulhammer et. al. [36]. The capsule filling process was accomplished with the lab-scale machine Labby (MG2, Bologna, Italy), which applies the dosator principle. Details to the machine can be found elsewhere [64]. The four blends were filled using two different settings with two different compression ratios, i.e. the ratio of dosing chamber length to the height of the powder layer (listed in Tab. 3).

Tab. 3: Specification of the capsule filling settings (CFS)

Setting	Dosator diameter [mm]	Dosing chamber length [mm]	Powder layer height [mm]	Capsules per hour [cph]	Compression ratio
CFS 1	3.4	2.5	5	2500	1:2
CFS 2	3.4	2.5	10	2500	1:4

With these settings a target fill weight of about 25 mg could be expected. The adhesive mixtures were filled by hand into the rotating container. The surface of the powder bed layer was smoothed by rotating the container manually and the layer height was checked with a vernier caliper. Afterwards capsule filling was executed for 30 min, whereas at time point 0 min, after 5 min, 10 min and 30 min about 30 capsules were sampled to analyse the fill weight and mixing homogeneity over time. During the whole process powder was repeatedly fed manually into the rotating container in order to compensate the loss of removed powder and to guarantee a steady powder bed height. The entire process was individually executed for each blend and each setting. For this, the powder layer was removed after each process, the apparatus was cleaned and afterwards new and unused blend was filled in the rotating container. All experiments were carried out under controlled environmental conditions (23.0 - 28.5 °C and 44 - 55% relative humidity). To evaluate the change in fill weight over time, the collected and filled capsules were weighed and the mass of the empty ones were subtracted to obtain the real fill weight. Moreover, the mixing homogeneities of the blends at each time point were analysed with HPLC. For this, three capsules (except of the time point when

powder retention was measured, see next paragraph; there nine capsules) were opened, the powder emptied and dissolved in buffer.

Since it was not possible to get the complete amount of powder out of the opened capsules, it was analysed how much powder was retained on the capsule shells. For this, two different methods were tested to determine the amount of remained SS on the capsule shells. For the first method, the emptied capsules were directly dissolved in buffer. For the second method, a cotton bud was soaked with buffer and the capsule shell was wiped out until no powder residue was visible anymore. The cotton bud was then held beyond a volumetric flask and rinsed with buffer. Three capsules of each blend, sampled after 5 min and filled with setting CFS 2, were used for each method. The SS content was subsequently analysed by HPLC.

2.7. Aerosolisation assessment

The aerosolisation performance of all four blends at both capsule fill settings was determined with a NGI (Copley Scientific, Nottingham, United Kingdom) and according to the procedure described in the Pharmacopoeia [65]. For all experiments, the capsules sampled after 30 min were used, since it was expected that after this time start up effects, occurring during capsule filling were completed (see section 3.4.) [70]. At first the vacuum pump (SCP5, Copley Scientific) was switched on and a coating agent (2% of Tween 20 in ethanol absolute), for coating the impaction trays, was produced. The small impaction trays were coated with 2 ml and the two larger ones with 4 ml, respectively. To guarantee that the coating agent was able to cure completely, 30 min were waited. After that, the individual parts of the NGI were assembled, 10 ml of buffer were filled in the pre-separator and the flow rate through the device was set to 100 L/min using a critical flow controller (TPK, Copley Scientific), which was checked with a flow meter (DFM3, Copley Scientific). Furthermore, the seal tightness of the apparatus was examined to ensure that the pressure inside the sealed NGI increased only by a maximum of 2.0 kPa within 60 seconds [36]. Afterwards the Aerolizer® was filled with a capsule and the assessment was started. For this, the capsule was pierced three times and the inhaler was connected via the mouthpiece of to the NGI. The solenoid valve of the flow controller was then opened three times for each capsule, every time for 2.4 sec., resulting in an air volume of 4 l that was sucked through the apparatus, respectively. For each run, three capsules were used in order to obtain a measureable amount of SS on each impaction tray. Subsequently, the inhaler and the capsules, the mouthpiece combined with the 90° inlet tube, and each of the eight trays were flushed with 10 ml buffer in order to dissolve the impacted SS particles at each stage. Additionally, 50 ml of buffer were added in

the pre-separator. The SS content was then analysed using HPLC. The whole assessment was done in triplicate for each blend and each setting.

2.8. HPLC method

The HPLC method was used for both, checking the mixing homogeneity of the blends as well as measuring the SS content in the NGI tests. The measurements were performed with a Waters 2695 (Milford, USA) with a column temperature of 30 °C, as described by Faulhammer et. al. [36]. As mobile phase, a mixture of methanol and an aqueous solution of 5 mM hexanesulfonic acid sodium salt with 1 % acetic acid, mixed in the ratio 2 to 3, were used. The stationary phase was a Phenomenex Luna C18 5 µm 100 Å column. 80 µl of the sample solutions were used for each HPLC measurement.

3. Results and Discussion

3.1. Particle characterization

This chapter comprises the measurement results of the solid state of the particles, the particle size distribution and the particle morphology.

3.1.1. Solid state of the particles

The solid state of LH100, JM SS and SD SS was confirmed by WAXS. The WAXS patterns of the three powders are displayed in Fig. 8 & 9.

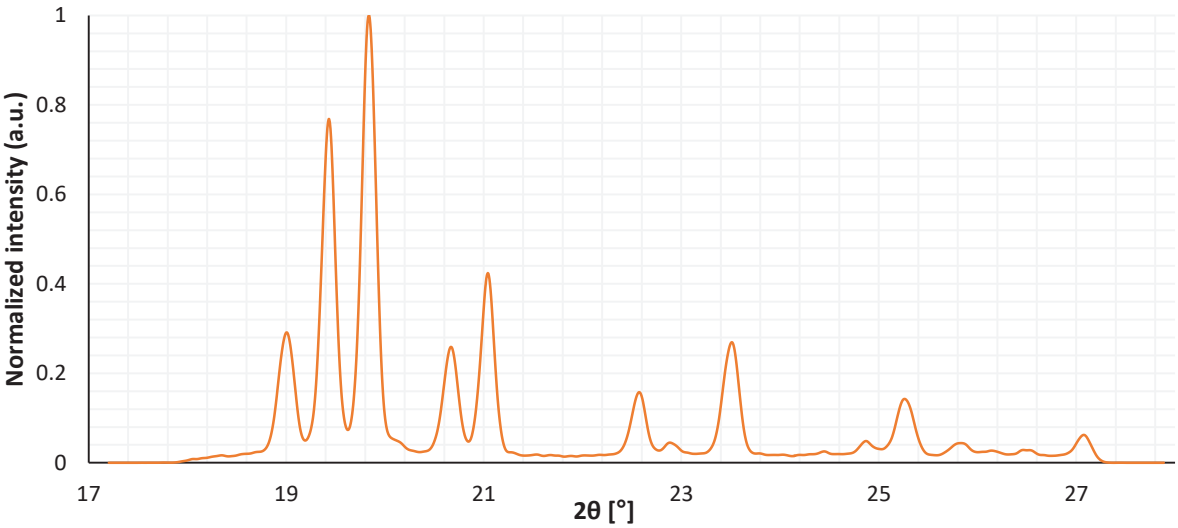

Fig. 8: WAXS pattern of the LH100

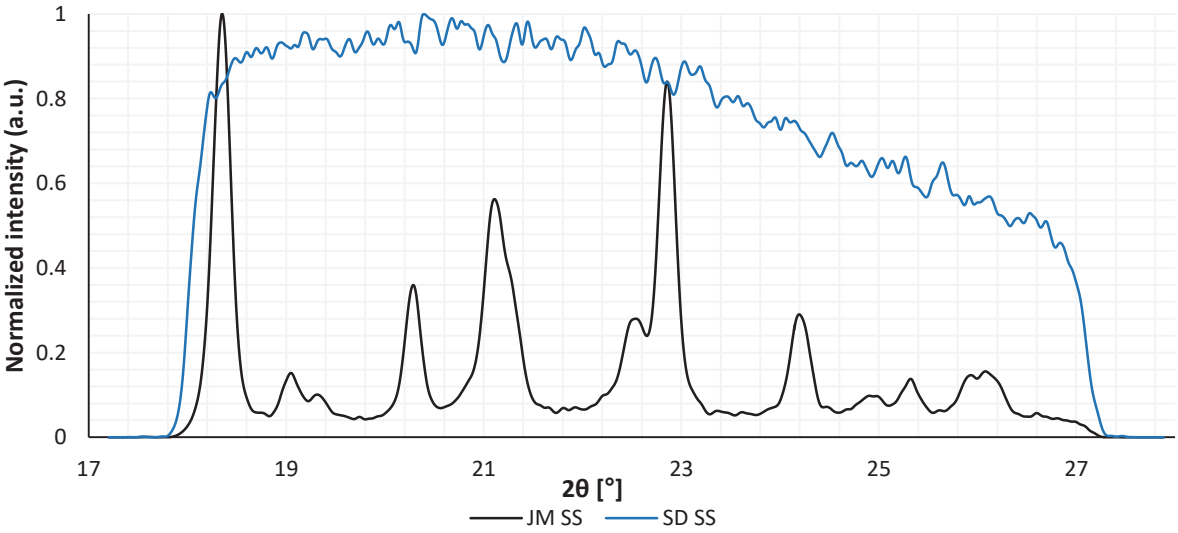

Fig. 9: WAXS pattern of JM and SD SS

The WAXS pattern of LH100, presented in Fig. 8, showed the typical peaks at 19.0°, 19.4° and 19.8° of crystalline lactose monohydrate [71]. In Fig. 9, the difference between amorphous and crystalline WAXS pattern of the SS can be observed. The pattern for JM SS displayed clear Bragg peaks, while that one of SD SS showed an amorphous halo, confirming that JM SS particles were crystalline and SD SS particles solidified in the amorphous state [72]. To guarantee that SD SS stayed in the amorphous state throughout further processing (blending, capsule filling) and storage, it was always kept at a relative humidity below 60%, to avoid recrystallization [73]. A further WAXS measurement of the high API load SD SS blend after capsule filling proved that the SD SS was still amorphous (patterns shown in the Appendix A., Fig. 24). The residual moisture content of the JM SS was 0.30 w% and that of the SD SS was 3.53 w%.

3.1.2. Particle size distribution

The important parameters used to describe the particle size distribution (PSD) and to compare the different distributions among each other were the $d_{v,10}$, $d_{v,50}$ and $d_{v,90}$. These values represent the particle's volume equivalent diameters where 10%, 50% or 90% of the measured powder bulk possess a smaller particle diameter. With these values, it is possible to determine the Span of a distribution in order to conclude if a distribution is hetero- or monodisperse. The Span defined as the difference of the $d_{v,90}$ and the $d_{v,10}$ divided by the $d_{v,50}$ [70]. All following PSDs are volume based (Q3), depicted as log normal distributions.

The parameters of the PSD of the carrier and the raw SS, before engineering, can be found in Tab. 4. The used primary pressure of the Rodos/L was 0.5 bar. The PSD of the carrier particles was in a similar size range to those one finds in literature, where adhesive mixtures were used for DPIs [19], [36]. The raw SS particles, however, were too large for pulmonary administration. The $d_{v,50}$ was larger than 5 µm and thus most of the particles were outside the aerodynamic size range.

Tab. 4: Parameters of the PSDs of the LH100 and the raw SS (n=3 ± SD)

Material	$d_{v,10}$ [µm]	$d_{v,50}$ [µm]	$d_{v,90}$ [µm]	Span
LH100	53.25 ± 0.26	120.91 ± 0.44	200.30 ± 1.32	1.22
Raw SS	1.86 ± 0.02	9.74 ± 0.03	25.26 ± 0.08	2.40

Consequently, second processing of the API particles was necessary. Two different batches were produced of the jet milled SS. The first one (batch 1) was used for the screening experiments and the second one (batch 2) for the scale up blends. Moreover, the effect of

sieving on PSD of the API was investigated with the JM SS (batch 2) and the SD SS. The powders were analysed at primary pressures of 0.1 and 0.5 bar and with the R2 and R5 lenses. Fig. 10, Fig. 11 and Fig. 12 display the size distributions of the JM SS (batch 1 & batch 2) and of the SD SS.

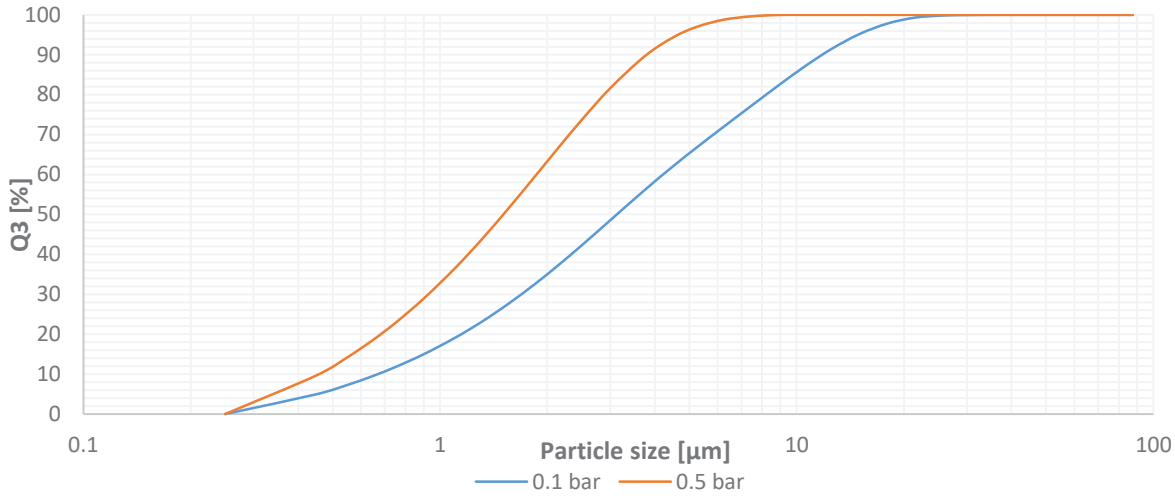

Fig. 10: PSDs of the JM SS (batch 1) at R2 (n=3)

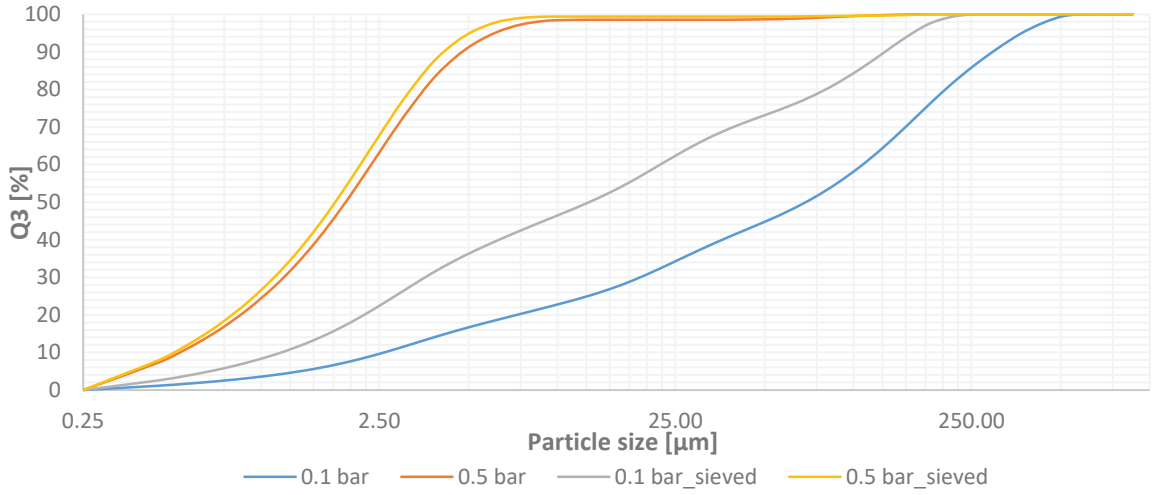

Fig. 11: PSDs of the JM SS (batch 2) at R2 & R5 before and after sieving (n=3)

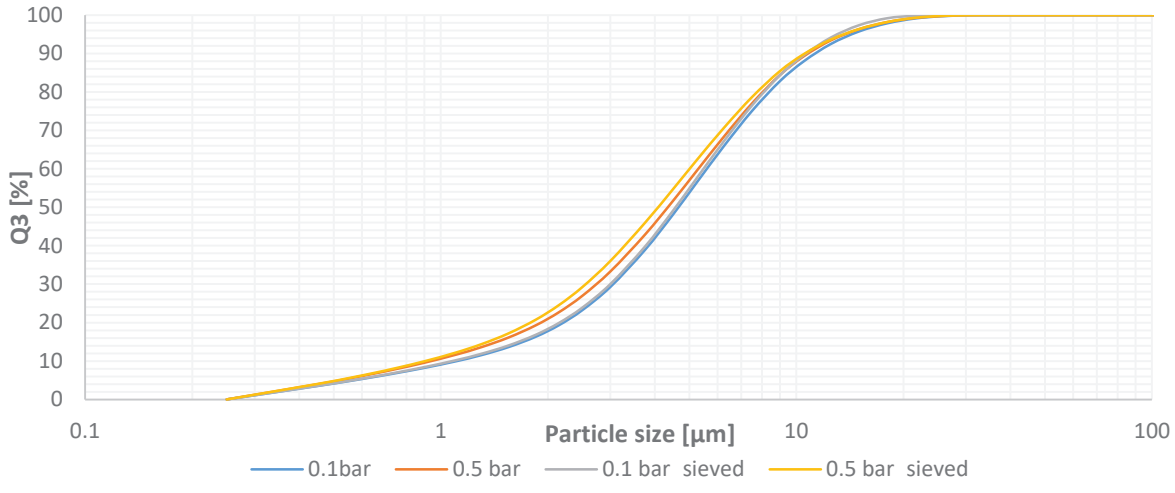

Fig. 12: PSDs of the SD SS at R2 & R5 before and after sieving (n=3)

With the figures above, it becomes clear that by means of jet milling and spray drying it was possible to reduce the particle size of the raw SS in order to obtain API particles in the aerodynamic size range, when an appropriate dispersion pressure of 0.5 was used [35]. In regards to the JM SS, a significant difference could be found when comparing the PSDs measured at different pressures (0.1 and 0.5 bar). At 0.1 bar larger particle sizes were observed, pointing out that API particle agglomerates not able to be broken up at this low pressure were present. By sieving, however, it was possible to partly break up these agglomerates as can be seen in the shift to smaller particle sizes at the lower primary pressure (Fig. 11). Consequently, it becomes evident that it is beneficial to sieve the JM SS before blending in order to obtain individual JM SS particles that are able to distribute homogeneously over the carrier surface and thus guarantee a homogeneous blend (see section 3.2.). In contrast to that, the PSD of the SD SS was neither influenced by different primary pressures nor by sieving. This, in turn, indicates that after particle engineering SD SS particles did not form agglomerates or only very few agglomerates of very small sizes which were able to pass through the sieve. The difference in agglomeration tendency of the two different engineered forms of SS could be partly explained by their different shapes. Flat JM SS particles exhibit higher contact areas and smaller interparticle distances, resulting in strong cohesion between the JM particles [40]. By contrast, for the SD SS particles the interparticle distances were much larger and the contact areas smaller, resulting in hardly any particle interaction. Due to the agglomeration tendency of JM SS and to be able to compare the absolute particle sizes of the two different engineered forms of SS, the results at the higher primary pressure were used, since this pressure was high enough to disperse the JM SS. The results show that JM SS (batch 1 & 2) displayed smaller particle sizes than SD SS. The width of the distributions at this primary pressure of 0.5 bar, however, was similar for both engineered forms (see Tab. 5).

Tab. 5: Parameters of the PSDs of the engineered forms of SS (n=3 ± SD)

Material	Condition	$d_{v,10}$ [µm]	$d_{v,50}$ [µm]	$d_{v,90}$ [µm]	Span
JM SS (batch 1)	0.1 bar/R2	0.67 ± 0.01	3.15 ± 0.08	11.85 ± 0.40	3.55
	0.5 bar/R2	0.46 ± 0.01	1.51 ± 0.03	3.82 ± 0.14	2.23
JM SS (batch 2)	0.1 bar/R2R5	2.60 ± 0.11	69.00 ± 2.04	296.23 ± 4.58	4.26
	0.5 bar/R2R5	0.53 ± 0.01	1.93 ± 0.09	4.89 ± 0.69	2.26
	0.1 bar/sieved/R2R5	1.17 ± 0.05	12.74 ± 1.69	127.92 ± 2.25	9.95
	0.5 bar/sieved/R2R5	0.51 ± 0.00	1.78 ± 0.01	4.18 ± 0.07	2.06
SD SS	0.1 bar/R2R5	1.11 ± 0.02	4.67 ± 0.03	11.38 ± 0.29	2.20
	0.5 bar/R2R5	0.94 ± 0.01	4.36 ± 0.04	10.83 ± 0.14	2.27
	0.1 bar/sieved/R2R5	1.08 ± 0.0.1	4.58 ± 0.04	10.66 ± 0.17	2.09
	0.5 bar/sieved/R2R5	0.91 ± 0.02	4.10 ± 0.12	10.58 ± 0.25	2.36

3.1.3. Particle morphology

Fig. 13 shows the particle shape of the used carrier particles. The tomahawk shape, which was already described in literature [74], [75] and which is typically for α-lactose monohydrate crystals, can be clearly seen. The particles exhibited predominantly plane surfaces, however, also areas with clefts and cavities could be found. Moreover, it is also visible that small fine lactose particles adhered to the surface of larger ones.

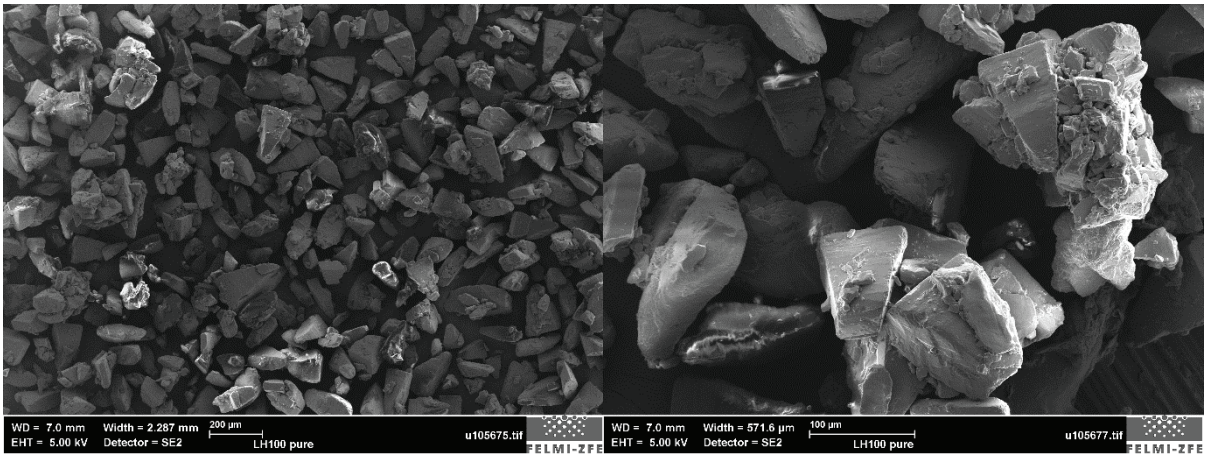

Fig. 13: Particle morphology of the used carrier LH100

The two engineered forms of the SS differed significantly from each other. The JM SS (Fig. 14) was very anisotropic. The particles showed elongated, needle-like shapes with angular borders. It is also observable that with jet milling produced particles exhibited different sizes and tended to form big agglomerates. The SD SS particles (Fig. 15), in contrast, were spherically shaped and hardly formed any agglomerates. Their surface was quite wrinkled, which was particularly striking for larger particles. This difference in the surface topography of spray dried particles is strongly dependent on the outlet temperature of the spray drier [76].

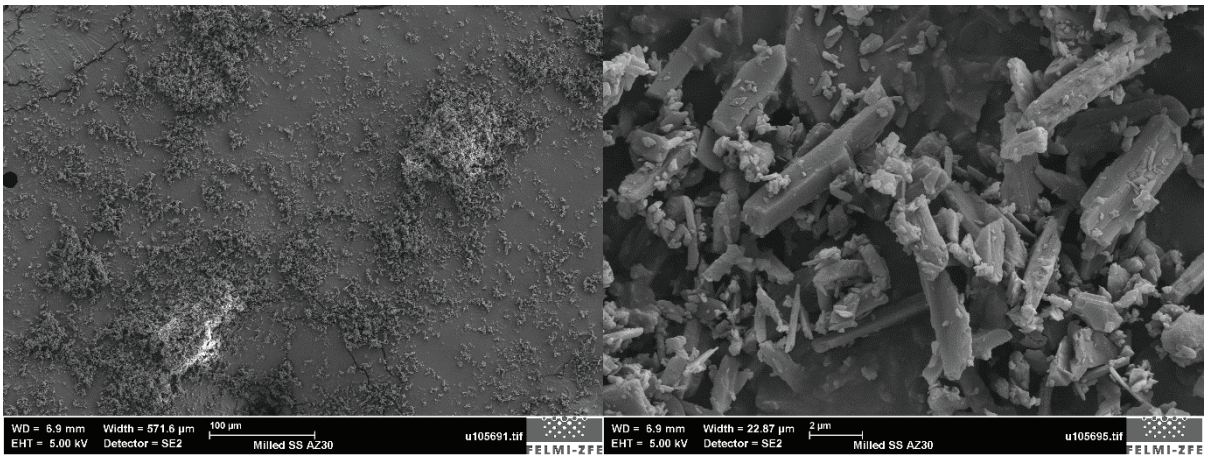

Fig. 14: Particle morphology of the JM SS

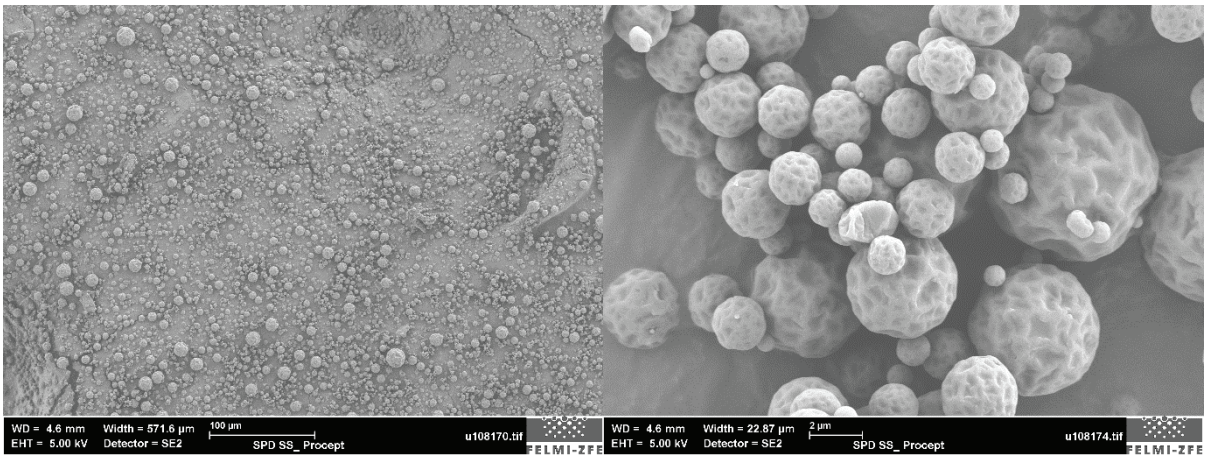

Fig. 15: Particle morphology of the SD SS

3.2. Powder blending

This chapter is divided into two subsections. First the experimental findings concerning the screening of the best mixing parameters are presented and subsequently the blending of the scale up blends is discussed. A thing that has to be mentioned already at the beginning of this chapter is that the used sampling method for analysing the mixing homogeneity was not the most adequate one. As a spatula was used for sampling, it was only possible to draw samples at certain points of the powder bulk. Moreover, this method could have introduced irritations inside the bulk, potentially leading to segregation. A better method would be to sample across the whole powder bulk. However, no adequate sampling equipment is available for this small scale.

3.2.1. Screening results of the mixing parameters

The screening of the mixing parameters was performed in two steps. First, only the mixing time and the rotational speed of the blender were altered. The aim was to find mixing conditions that provided blends with mixing homogeneities with a RSD below 15%. This limit was chosen, since it was presumed that by means of sieving of the API and mixing at a reduced filling ratio (RFR), it would be possible to improve the mixing homogeneity from a RSD value of 15% to a RSD below 5%.

Tab. 6: Screening results of the mixing conditions

Mixing condition	API load	RSD < 15 %
MC 1	1%	✗
MC 1	10%	✗
MC 2	1%	✗
MC 2	10%	✗
MC 3	1%	✗
MC 3	10%	✗
MC 4	1%	✓
MC 4	10%	✓

In Tab. 6 it is shown that only the combination of a long mixing time (90 min) and a high rotational speed (90 rpm) made it possible to produce blends with mixing homogeneities with a RSD < 15%, regardless if a low or high API load was used. This could be explained by the fact that a longer mixing time enhances the press on forces and a higher rotational speed leads to a sufficient break-up of the API agglomerates, both things promote the production of homogeneous adhesive mixtures, as already described in section 1.4.3. Therefore, the remaining three mixing conditions (MC 1 – MC 3) were already rejected at this point. The objective of the second screening step was then to use MC 4 and to try two further measures (sieving of the SS and a RFR) in order to obtain homogeneous mixtures with a RSD < 5%. The theoretical description why these two measures could improve the mixing homogeneity can be found in section 2.4.1.

Tab. 7: Screening results (with sieving of SS and RFR)

Mixing condition	API load	Sieved SS	RFR	RSD < 5 %
MC 4	1%	no	no	✓
MC 4	1%	yes	no	✓
MC 4	10%	no	no	✗
MC 4	10%	yes	no	✗
MC 4	10%	no	yes	✗
MC 4	10%	yes	yes	✓
MC 5	1%	yes	no	✓
MC 5	10%	yes	yes	✓

Tab. 7 summarises the effects of sieving and RFR on mixing homogeneity. For the low API load blend it did not make any difference, whether the SS was sieved or not, since in both cases it was possible to produce homogeneous mixtures. This implies for the low API load blend that forces, arising during mixing, were high enough to break up API agglomerates and a homogeneous API distribution was obtained. Due to that reason, this blend was not mixed at RFR. In contrast, for the high API load blend neither sieving of the SS nor mixing at RFR

provided homogeneous mixtures. Consequently, it seems that in this high API load blends strong mixing forces are needed to break up the drug agglomerates and to distribute the API consistently within the adhesive mixture. So only the combination of sieving and a RFR yielded in homogeneous adhesive mixtures. Although for both API loads, good procedures were found in order to ensure adequate mixing homogeneities, a further improvement was tested. Since it is always the aim to find the briefest mixing time and the lowest rotational speed able to produce homogeneous blends. Moreover, shorter mixing times and lower mixing speeds could potentially result in weaker press on forces and thus enhance API detachment during inhalation [20]. Hence, a new mixing condition (MC 5, Tab. 1) was tried out. It was an intermediate of all other mixing conditions and as can be seen in Tab. 7 it made the production of homogeneous adhesive mixtures possible, for both the low and high API load.

To summarise the whole screening, it can be stated that the best mixing condition for the scale up blends were found to be MC 5, with a mixing time of 47.5 min. and a rotational speed of 55 rpm. Additionally, the SS should be sieved before mixing and the high API load blend should be mixed at a reduced filling ratio.

3.2.2. Mixing homogeneity of the up-scaled blends

The four up-scaled blends (listed in Tab. 2) were mixed with the mixing conditions described in the previous section. Mixing homogeneity results of all four can be found in the subsequent table (Tab. 8).

Tab. 8: API content and mixing homogeneity of the up-scaled blends

Specification	API content	Mixing homogeneity (RSD)
Blend 1	0.98 ± 0.02 %	1.70 %
Blend 2	9.46 + 0.41 %	4.32 %
Blend 3	0.94 ± 0.05 %	5.15 %
Blend 4	8.43 ± 0.98 %	11.60 %

The blends with JM SS showed better mixing homogeneities than those with SD SS. To draw conclusions and explain why it came to these differences between the two engineered forms of SS, SEM images were taken from all blends (Fig.16 – 19). Although SEM images only display an unrepresentative amount of particles, they are suitable to draw conclusions about adhesive mixing, particle interaction and bulk properties [36].

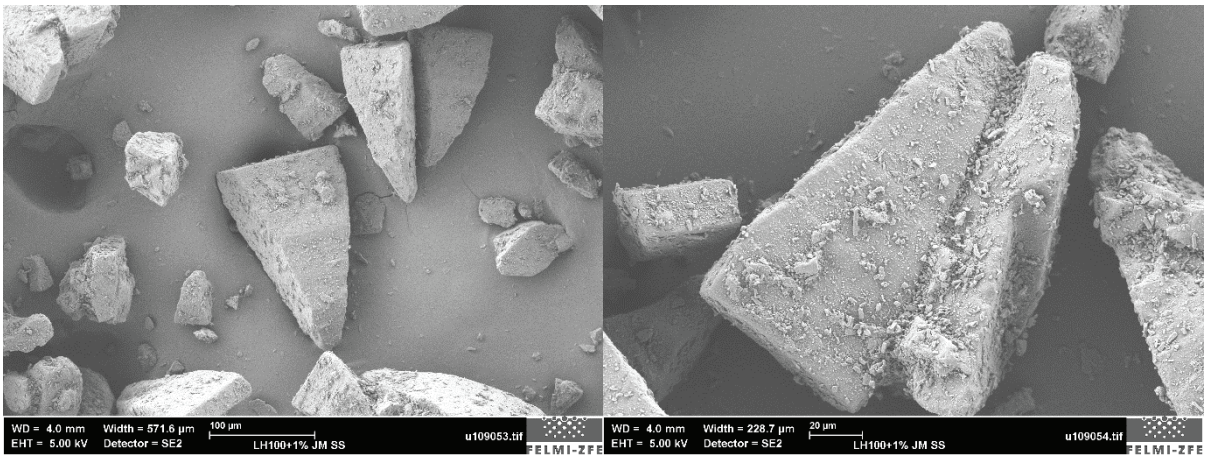

Fig. 16: SEM image of blend 1

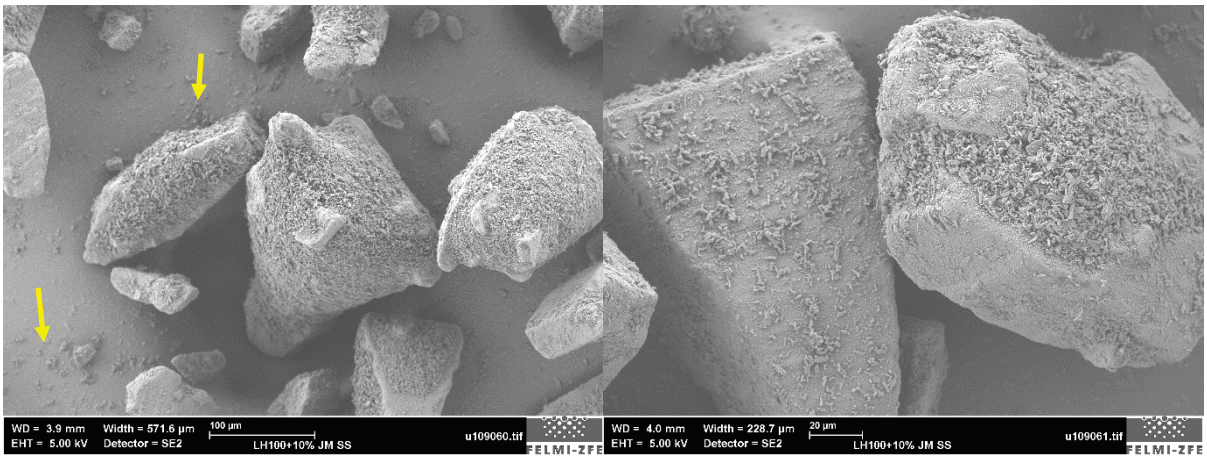

Fig. 17: SEM image of blend 2

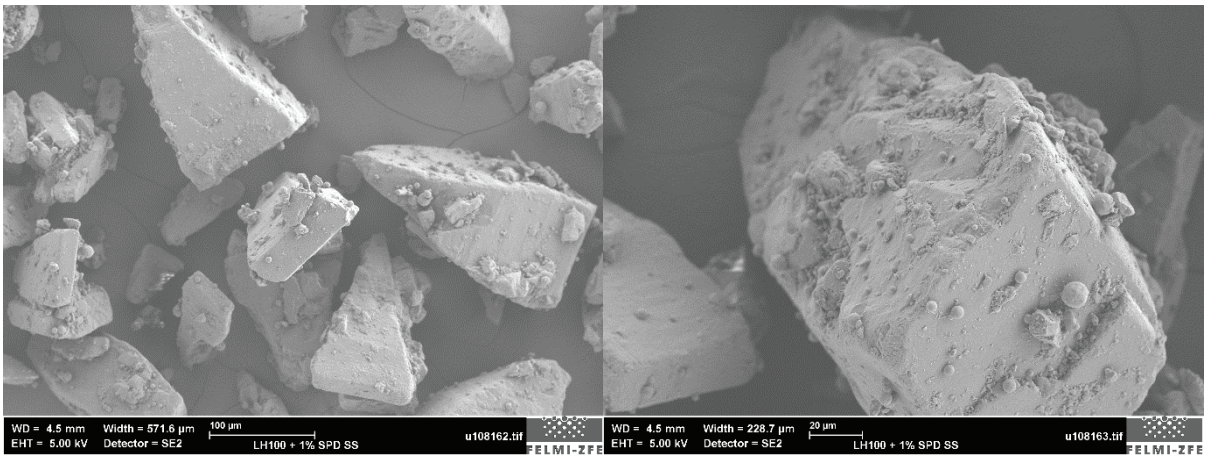

Fig. 18: SEM image of blend 3

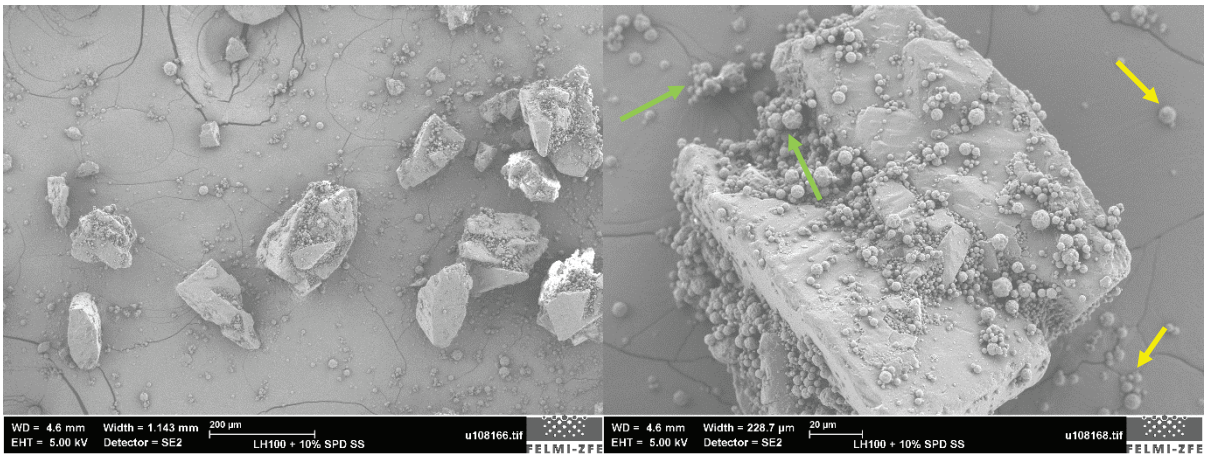

Fig. 19: SEM image of blend 4

The API particles of the low API load SS (JM & SD) blends were distributed very homogeneously over the carrier surface. This was also confirmed by the results of the mixing homogeneity. Blend 1 showed the best mixing homogeneity, whereas the mixing homogeneity of blend 3 was slightly above the 5% limit. However, when one takes the bad sampling technique (described in section 3.2.) into account, one can argue that the mixing homogeneity of blend 3 is still satisfying. The high API load blends differed more significantly. It was apparent that for this API load, parts of the carrier surface was already saturated with API particles. This caused on the one hand a partly multilayer formation of API particles on the carrier surface, resulting in API-API interaction instead of API-carrier interaction, and on the other hand loose, not attached API particles (see yellow arrows in Fig. 17 & 19). It has already been investigated in literature that higher carrier payloads reduce the adhesion forces between API and drug particles [41]. The latter was especially true for the SD SS as can be clearly seen in Fig. 19 and it consequently represents a reason for the bad mixing homogeneity of blend 4. Since it might have happened that these loose API particles segregated and accumulated at the corners on the bottom of the mixing container, where they could not be sampled with the used sampling technique. These circumstances could also clarify the difference in expected (10%) and measured API content of blend 2 and 4 (see Tab. 8). The different distribution of JM and SD SS particles over the carrier surface in the high API load blends was also striking. JM SS was distributed very homogeneously over the whole carrier. Only the edges of the carrier were hardly covered with JM SS particles (what makes sense as during mixing only marginal press on forces act on these positions). The SD SS particles, by contrast, were preferably attached to the asperities (i.e. clefts, cavities) of the carrier surface and only a little amount of the API particles were found on the plane surfaces. This might be explained by the fact that adhesive forces are higher in these asperities than on the plane surfaces of the carrier. Furthermore, shear forces, arising during mixing, could have been strong enough to detach the SD SS particles form the plane

surfaces of the carrier, resulting in a redistribution to the asperities where they were hardly affected by those forces. It seems also that parts of SD SS particles agglomerated, both in the carrier irregularities and also apart from the carrier surface (see green arrows in Fig. 19). These agglomerates probably formed during mixing, since it was proved by PSD measurements (section 3.1.2.) that no SD SS agglomerates were present after particle engineering. This agglomeration effects of API particles during mixing has been already investigated by Grasmeijer et. al. [77]. Furthermore, the author observed that the amount and size of the API agglomerates correlate with the API load in the blend [78]. Later on when evaluating the aerodynamic performance of the blends, one should take all these findings, mentioned in this paragraph, into account.

3.3. Powder bulk properties of the blends

Powder bulk, friction and flowability properties of the pure LH100 as well as of all four adhesive mixtures were investigated using the FT4 powder rheometer. The results of the measurements are summarised in the following three subsections.

3.3.1. Shear cell testing

This measurement allows to determine the flow function coefficient (FFC) of a powder bulk. It is represented as the ratio between consolidation stress and unconfined yield strength. Easy flowing powders show FFC values larger 4 [79]. Additionally, the cohesion coefficient (Coh. Coeff.), described as the shear strength when no normal stress is applied, and the angle of internal friction (AIF) that denotes the angle between the yield locus and the abscissa, were determined and are listed in Tab. 9.

Tab. 9: Overview shear cell measurement results (n=3 ± SD)

	Coh. Coeff. [kPa]	FFC	AIF [°]
LH100	0.21 ± 0.02	7.08 ± 0.75	17.54 ± 0.88
Blend 1	0.19 ± 0.01	7.58 ± 0.52	19.86 ± 0.93
Blend 2	0.32 ± 0.02	4.87 ± 0.29	22.31 ± 0.91
Blend 3	0.22 ± 0.01	7.00 ± 0.08	15.47 ± 0.29
Blend 4	0.27 ± 0.01	5.67 ± 0.19	15.83 ± 0.81

FFC values show that all blends should flow easily, however, it is distinct that blends with the low API load flowed better than those with the high API load. This is also confirmed by the cohesion results. Blend 1 and 3 showed similar values as pure LH100, whereas blend 2 and

blend 4 were more cohesive. In regards to the AIF findings, it is obvious that JM SS blends showed higher and SD SS lower values than pure LH100. This might be due to the different shapes of the two engineered API forms. The spherical shaped SD SS particles could have acted as a glidant, reducing the friction between the coarse carrier particles and thus resulting in lower values for the AIF. This was already obtained by Podczeck and Miah, who observed that anisotropic particles show higher values for the AIF [80].

3.3.2. Aeration testing

With the aeration method, three properties were measured. The (1) basic flowability energy (BFE) represents the amount of work needed to stir a blade in a circular motion through a conditioned static powder bed. If the powder bulk is perfused by air and finally gets completely fluidised, flow energy decreases to a steady value, the (2) aerated energy (AE). The ratio of the former two parameters is described as (3) aeration ratio (AR) [58]. That implies that the lower the AE and the larger the AR the easier a powder bulk is aerated and the less cohesive it is. AR is often the parameter of choice to compare different powders with each other. AR values above 20 indicate powder bulks that show high tendency to become fluidised [69].

Tab. 10: Overview aeration measurement results (n=3 ± SD)

	BFE [mJ]	AE [mJ]	AR
LH100	588.71 ± 8.73	3.85 ± 0.20	153.38 ± 10.27
Blend 1	733.28 ± 6.15	2.04 ± 0.47	375.35 ± 84.85
Blend 2	930.12 ± 50.49	91.08 ± 13.90	10.35 ± 1.50
Blend 3	262.67 ± 36.71	2.46 ± 0.71	113.35 ± 37.51
Blend 4	115.45 ± 11.56	3.16 ± 0.64	37.50 ± 7.65

The AR values in Tab. 10 show clearly that the blends with the high API load were more cohesive and became much worse aerated than those with low API loads. This could be due to the higher amounts of fine particles in the blend, as already described by Cordts and Steckel (2012) [81]. In principle, however, all powders were fluidised very easily, except of the high API content JM SS blend (blend 2), which exhibited only a moderate tendency to be fluidised. This trend was also indicated by the measurement results of the AE. Thus, it can be concluded that blend 2 was much more cohesive than the other ones, which can be correlated to the high amount of micronized particles and to the results of the cohesion coefficient in section 3.3.1.

3.3.3. Air permeability testing

The air permeability of a powder bulk is usually quantified with the pressure drop (Δp) that arises when air is passed through. In theory, low values of Δp display highly porous powder bulks that have good capabilities to transmit air. For the permeability testing, Δp was determined for different compression states of the powder bulk and at a constant air flow rate of 2 mm/s (Fig. 20).

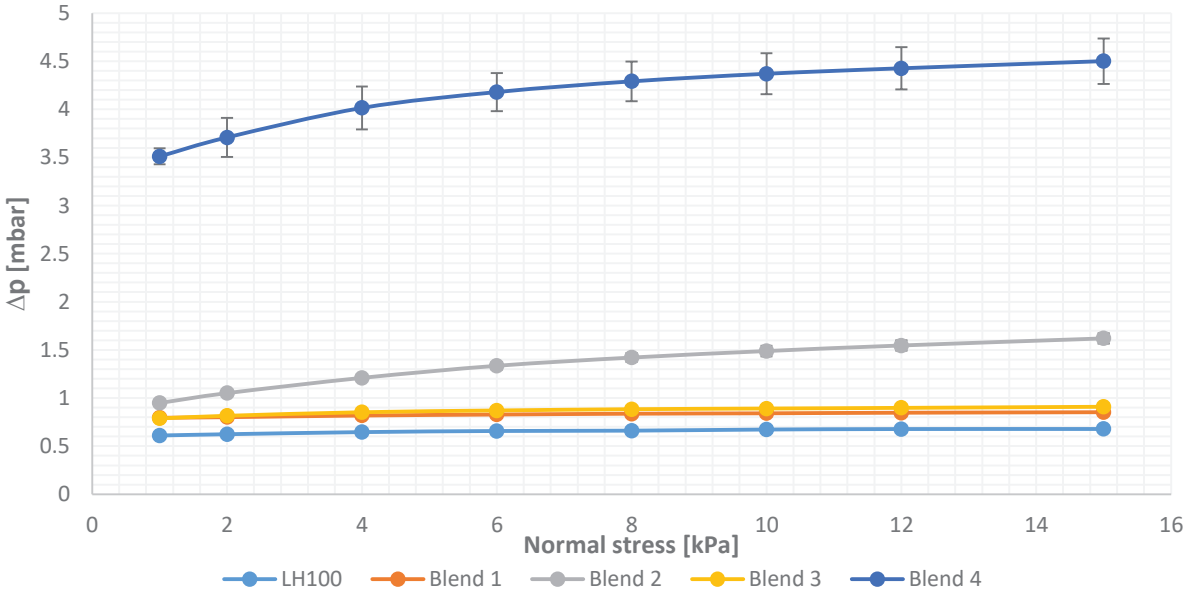

Fig. 20: Air permeability results of the different blends (n=3 ± SD)

The low API load blends (blend 1 & 3) displayed pressure drops approximately similar to that one of pure LH100 and were not influenced by different compression states. For the high API load blends it looked different, they exhibited higher Δp, whereas that one of blend 4 was considerably higher. It could be hypothesised that the higher amount of fine particles in those two blends is responsible for the higher Δp. As already mentioned in section 3.2.2., in blend 4 appeared a high amount of loose SD SS particles. These spherical and soft particles could potentially accumulate in the voids between the carrier particles, increasing the resistance to the airflow and thus increasing the Δp over the powder bulk. This became more significant at increased compression states, proposing that porosity of the powder bulk steadily decreased [81].

3.4. Capsule filling

First of all, it has to be mentioned that for none of the four blends any difficulties occurred during all capsule filling trials. All adhesive mixtures were easy to fill with the Labby capsule filling machine. Each adhesive mixture formed a uniform powder bed layer, no empty capsules were ejected and no powder plugs were formed, which is desirable for DPIs (see section 1.5.1.). The only striking thing that appeared was that already after the filling process, parts of the adhesive mixture attached to the capsule walls. In the following three subchapters, the filling performance of the four blends as well as the measurement results concerning powder retention on the capsule shells are summarised.

3.4.1. Capsule filling of the JM SS blends

In Tab. 11 the fill weights of the JM SS blends for both capsule filling settings are displayed. It is obvious that, regardless which adhesive mixture and which capsule filling setting was used, the fill weight variability at each time point was only marginal. This, in turn, indicates that blend 1 & 2 were suitable to be filled with the dosator principle. Regarding the different settings, it was found that a higher compression ratio (CFS 2) resulted in a higher fill weight. This finding makes sense, since a higher compression ratio causes a densification of the particles inside the powder bulk, leading to a larger mass of particles per unit volume and thus to a higher capsule fill weight. The API load, however, had no distinct influence on latter. For CFS 1 the API load had almost no effect, yet, for CFS 2 a slightly higher fill weight was achieved with the high API load blend. Moreover, concerning capsule fill weight over time, no clear trend could be obtained. Only for blend 1/CFS 2 a considerable difference in fill weight between time point 0 min and the remaining time points can be marked. This might be due to a compaction process of the powder layer over time, which is caused by vibrations of the capsule filling machine, as already described by Stranzinger et. al. [70]. The minor variation in fill weight over time of the other trials was most likely caused by the matter of fact that the dosator does not always collect the same quantity of powder and by variations in manual feeding. Since the powder was repeatedly fed by hand into the rotating container to compensate the loss of powder (see section 2.6.), it could happened that not always the same amount of powder was filled in the container which possibly influenced the powder bed and thus resulted in the slight variation of the fill weight over time.

Tab. 11: Capsule fill weight and mixing homogeneity results over time of JM SS blends

		0 min	5 min	10 min	30 min
Blend 1 / CFS 1	Fill weight [mg] (± RSD [%])	21.8 (± 1.76)	22.1 (± 1.31)	22.2 (± 1.08)	22.7 (± 1.42)
	Mixing homogeneity (RSD [%])	1.66	3.81	2.75	2.44
Blend 1 / CFS 2	Fill weight [mg] (± RSD [%])	22.6 (± 1.36)	24.0 (± 1.08)	24.1 (± 1.43)	24.2 (± 1.17)
	Mixing homogeneity (RSD [%])	1.27	2.38	2.65	2.44
Blend 2 / CFS 1	Fill weight [mg] (± RSD [%])	22.4 (± 1.61)	22.5 (± 1.50)	22.1 (± 2.31)	21.3 (± 2.21)
	Mixing homogeneity (RSD [%])	4.24	6.95	8.36	5.48
Blend 2 / CFS 2	Fill weight [mg] (± RSD [%])	25.1 (± 1.64)	25.7 (± 1.11)	25.8 (± 1.03)	25.4 (± 0.94)
	Mixing homogeneity (RSD [%])	10.95	14.48	15.14	9.57

Tab. 11 comprises also the results concerning mixing homogeneity during capsule filling. Capsules filled with blend 1 exhibited good mixing homogeneities. The RSD was below 5% at all time points and for both settings, indicating that blend 1 was a stable mixture that retained the same good mixing homogeneity as after blending. In contrast to that, the mixing homogeneity of blend 2 became worse compared to that one after blending, especially for the setting CFS 2. It might be that blend 2 was not that stable. In this blend, JM SS particles formed a multilayer on the carrier, resulting in weaker API-carrier interaction, as already described in section 3.2.2. Consequently, it could be that JM SS particles partially separated from the carrier surface during storage, transport and later on when the blend was filled in the capsule filling machine or even during capsule filling. Then it might be that these separated particles were distributed inconsistently throughout the powder bulk. This inconsistent distribution is more substantial for a higher powder bed, as it was set in CFS 2, since more space (volume) is available where these separated particles could spread. This might be the reason for the worse mixing homogeneity of blend 2 at setting CFS 2.

3.4.2. Capsule filling of the SD SS blends

As for the JM SS blends also for the SD SS blends the fill weight at the distinct time points hardly varied. This, in turn, implies that also blend 3 & 4 were appropriate to be filled with a dosator. In conclusion, it seems that dosator capsule filling is suitable for various adhesive mixtures with different API loads. Compared to blend 1 & 2, the capsule fill weight of the SD SS blends differed by a few grams. This was mainly caused due to the variation in the manual adjusting of the powder bed height and the dosing chamber length, since they were readjusted for each capsule fill run. Blend 3 resulted in a slightly lower fill weight than blend 1, while blend 4 resulted in higher ones than blend 2. The variability of the fill weight over time of the individual trials could be again caused due to the ongoing compaction process of

the powder bed, the variations in manual feeding and the variation in powder collection of the dosator, as described in section 3.4.1. The latter was especially true for blend 4 and the larger powder bed height, since compaction is more critical for higher powder bed layers [70]. This could be again related to the high amount of loose SD SS particles in the adhesive mixture. Due to vibrations during capsule filling, it could be that those particles accumulate in the voids of the powder bulk, leading to an ongoing densification and thus a higher fill weight. Similar to the JM SS blends, also for the SD SS ones, higher compression rates caused a higher fill weight. This might be again explained with the same reasons as mentioned in section 3.4.1. Additionally, the API load in the SD SS blends had also an impact on the fill weight. Capsules filled with blend 4 were heavier on average than those filled with blend 3, no matter which setting was used. This can be correlated to the higher cohesion and lower FFC of the high API load blend, listed in Tab. 9. It might also be explained by the fact that blend 4 exhibited a powder bulk, which was per se already denser and less porous, due to the mentioned loose SD SS particles, than that one of blend 3. Which, in turn, could be correlated to the high difference in air permeability of the two blends (see section 3.3.3).

Tab. 12: Capsule fill weight and mixing homogeneity results over time of SD SS blends

		0 min	5 min	10 min	30 min
Blend 3 / CFS 1	Fill weight [mg] (± RSD [%])	21.6 (± 3.46)	21.4 (± 2.08)	21.3 (± 2.00)	22.4 (± 2.35)
	Mixing homogeneity (RSD [%])	11.43	8.14	4.30	2.03
Blend 3 / CFS 2	Fill weight [mg] (± RSD [%])	21.4 (± 2.67)	23.2 (± 2.02)	23.0 (± 1.27)	23.2 (± 1.37)
	Mixing homogeneity (RSD [%])	7.61	4.61	4.89	7.07
Blend 4 / CFS 1	Fill weight [mg] (± RSD [%])	24.2 (± 2.13)	24.8 (± 1.33)	24.9 (± 1.86)	24.4 (± 1.65)
	Mixing homogeneity (RSD [%])	2.43	5.88	8.55	17.59
Blend 4 / CFS 2	Fill weight [mg] (± RSD [%])	24.9 (± 1.52)	26.1 (± 1.55)	26.8 (± 1.35)	29.7 (± 2.18)
	Mixing homogeneity (RSD [%])	11.66	4.98	13.21	9.68

Both SD SS blends exhibited per se a mixing homogeneity with a RSD beyond 5%. As a consequence, it was not surprising that the mixing homogeneities after capsule filling were also bad. The mixing homogeneities of the low API load SD SS blends were worse compared to those of the JM SS blends. And also those of the high API load SS blends were on average beyond the 5% limit. Overall it was observed that the mixing homogeneities fairly varied over time. For the setting with the small powder bed height (CFS 3), contrary trends of the mixing homogeneity of the two blends appeared over time. The mixing homogeneity of blend 3 was improved, while that one of blend 4 became worse over time. As opposed to this, CFS 2 caused no clear trend on the mixing homogeneity over time. It could be hypothesised that based on the substantial variation of the mixing homogeneity over time

that the adhesive mixtures with SD SS were not stable, as already described for blend 2. However, to draw a thorough conclusions further research has to be done in future.

3.4.3. Powder retention

Additionally to analysing the mixing homogeneity and the capsule filling performance, it was also investigated how much powder remained on the capsule shells when the capsule was just opened and the powder emptied. The results are listed in Tab. 13 & 14. The two methods used for powder retention measurements (see section 2.6.) are abbreviated as M 1 & 2. Whereas, M 1 is the capsule method and M 2 is the cotton bud method.

Tab. 13. Powder retention results of the low API load blends (n=3 ± SD)

	SS cont. pow. [mg]	SS cont. cap. [mg]	SS cont. pow. [%]	SS cont. cap. [%]
Blend 1/M 1	196.95 ± 3.01	74.28 ± 5.66	72.63 ± 1.55	27.37 ± 1.55
Blend 1/M 2	188.18 ± 3.13	20.99 ± 2.15	89.98 ± 0.77	10.02 ± 0.77
Blend 3/M 1	143.54 ± 7.30	94.92 ± 6.58	60.19 ± 2.69	39.81 ± 2.69
Blend 3/M 2	152.16 ± 3.83	30.99 ± 3.36	83.08 ± 1.77	16.92 ± 1.77

First, it has to be mentioned that both methods were not very suitable to measure the powder retention of the low API load blends. The SS content found in the powder (SS. cont. pow.) and capsule (SS cont. cap.) using the capsule method was higher than the theoretically detectable quantity (except blend 3/M 1, data is shown in the appendix, Tab. 17). This could be due to an interaction of the SS with the capsule material when both are in solution, which potentially affected the HPLC analysis. With the cotton bud method, on the other hand, less SS than the theoretically detectable quantity was found. This might be explained by two reasons: (1) with the cotton bud it was not possible to get the whole amount of SS out of the capsule shell and/or (2) a certain amount of SS remained in the cotton bud, after it was rinsed with buffer. Nevertheless, when one compares the relative retained amount of SS, it can be said that, no matter which method was used, a higher percentage of SD SS remained on the capsule shell compared to JM SS.

Tab. 14: Powder retention results of the high API load blends (n=3 ± SD)

	SS cont. pow. [mg]	SS cont. cap. [mg]	SS cont. pow. [%]	SS cont. cap. [%]
Blend 2/M 1	2311.05 ± 15.10	287.67 ± 13.59	88.93 ± 0.49	11.07 ± 0.49
Blend 2/M 2	2256.22 ± 29.41	144.45 ± 33.75	93.98 ± 1.39	6.02 ± 1.39
Blend 4/M 1	1214.63 ± 37.42	1073.40 ± 48.81	53.09 ± 1.22	46.91 ± 1.22
Blend 4/M 2	1179.62 ± 83.20	732.15 ± 38.31	61.66 ± 2.83	28.34 ± 2.83

For the high API load blends the used methods were more suitable, which could be correlated to the higher amount of API within these blends. For instance the interaction between the capsule material and the SS is less crucial than for the low SS load. However, again both methods provided measurement results of the SS amount that slightly differed from the theoretically detectable quantity (except blend 2/M 1, data is shown in the appendix, Tab. 18). As for the low API load blends it is also obvious for the high API load blends that relatively more SD SS remained inside the capsules than JM SS.

Based on the results and the fact that the used methods were not that appropriate, it is hard to draw a coherent conclusion, why relatively more SD SS remained in the capsule than JM SS. Moreover, one should always keep in mind that the powder retention results listed above were based on the powder that remained inside the capsules, when the powder was just emptied and not on the powder retained in the capsule after inhalation. Therefore, it would be advisable for further studies to determine the powder retention on the capsule shells after inhalation, since this is more relevant for DPIs. However, to obtain accurate results, the two mentioned methods should be improved or another method should be invented.

3.5. Aerosolisation performance of the blends

The airflow through the NGI was set to 100 L/min, as already mentioned in section 2.7. Using formula (2), it became possible to calculate the cut off diameters of the individual stages for this flow rate, which are summarised in Tab. 15.

Tab. 15: Cut-off diameters of the individual stages at a flow rate of 100 L/min

Stage 1	Stage 2	Stage 3	Stage 4	Stage 5	Stage 6	Stage 7	MOC
>6.12 µm	6.12 – 3.42 µm	3.42 – 2.18 µm	2.18 – 1.31 µm	1.31 – 0.72 µm	0.72 - 0.40 µm	0.40 - 0.24 µm	<0.24 µm

Values listed in Tab. 15 make clear that all particles, which deposited in stage 3 and the stages below as well as around 58.5% of the mass of SS deposited in stage 2, contributed to the fine particle dose (FPD). The 58.5% represented the portion of SS particles within a size range of 5.00 – 3.42 µm of the entire stage 2.

Tab. 16 includes the parameters describing the aerodynamic performance of the four blends at both capsule filling settings. The emitted dose (ED) was for all blends and both settings (expect of Blend 3/CFS 2) below the theoretically possible amount of SS, which implies that a considerable amount of SS remained in the capsules or was already deposited in the

inhalation device. For the individual blends, a correlation could be found between the emitted dose (ED) and the used capsule filling setting, when neglecting the high SD in some cases. Capsules filled at CFS 2 exhibited a higher fill weight and on average also higher EDs. This was particularly evident for blend 4. As can be seen in Tab. 12, the fill weight of the blend 4 capsules used for NGI assessment varied by more than 5 mg, depending on the setting which was used. This, in turn, explains the huge difference in ED between blend 4/CFS 1 and blend 4/CFS2. However, since the aerodynamic performance of blends with different API loads filled at different settings was analysed, the fine particle fraction (FPF) was used to compare the measurement results among each other. In total, it is obvious that the JM SS blends exhibited overall substantially higher FPDs than the SD SS ones, although, the EDs of the JM SS blends were quite similar or even lower compared to those of the SD SS ones. The highest FPF was found for the high API load JM SS blend (blend 2) and setting CFS 2. In principle, higher API loads showed higher FPFs. For the JM SS blends a trend could be observed between the powder bed height during capsule filling and the FPFs that is absent in the standard deviation (i.e. a higher powder bed enhanced the FPF). This trend was obvious for the low and high API load blend (blend 1 & 2). Whereas, the capsule fill setting had no considerable effect on the FPF of the SD SS blends. Reasons for all those findings will be explained in the subsequent paragraphs.

Tab. 16: Aerodynamic performance results of the four blends at CFS 1 & 2 (n=3 ± SD)

	ED [µg]	ED [%]	FPD [µg]	FPF [%]	MMAD [µm]
Blend 1/ CFS 1	408.40 ± 44.94	65.76 ± 2.49	88.18 ± 7.20	21.70 ± 2.14	2.64 ± 0.19
Blend 1/ CFS 2	512.54 ± 23.01	71.33 ± 2.03	152.23 ± 17.62	29.73 ± 3.59	2.35 ± 0.21
Blend 2/ CFS 1	5074.14 ± 1536.93	85.20 ± 9.82	2828.02 ± 1530.97	53.55 ± 12.89	1.63 + 0.20
Blend 2/ CFS 2	5764.36 ± 476.63	85.04 ± 2.01	3633.21 ± 526.62	62.82 ± 3.77	1.65 ± 0.15
Blend 3/ CFS 1	535.77 ± 25.52	82.12 ± 15.43	51.90 ± 13.74	9.66 ± 2.36	8.13 ± 1.39
Blend 3/ CFS 2	552.22 ± 16.62	100.00 ± 0.00	48.76 ± 6.18	8.83 ± 1.08	7.59 ± 0.82
Blend 4/ CFS 1	5094.86 ± 305.98	76.12 ± 0.58	1094.45 ± 62.69	21.58 ± 2.59	5.68 ± 1.36
Blend 4/ CFS 2	7051.71 ± 943.67	77.17 ± 2.83	1450.19 ± 107.92	20.93 ± 4.27	7.22 ± 2.22

The worse aerodynamic performance of the SD SS blends compared to that one of the JM SS blends is based on several reasons. A parameter that strongly influenced the difference in FPF between the two engineered forms of SS blends was the particle size. As mentioned in section 3.1.2., JM SS particles exhibited smaller diameters than SD SS particles. The $d_{v,50}$ measured via laser diffraction for sieved JM SS (batch 2) at a primary pressure of 0.5 bar, was 1.78 ± 0.01 µm, while that one of SD SS at the same setting was 4.10 ± 0.12 µm. This implies that a higher percentage of the PSD of the JM SS were in the inhalable size range, resulting in more particles able to penetrate down into the lower stages of the NGI and thus increasing the FPD. The difference in particle size was also clearly confirmed by the measurement results of the MMAD (Tab. 16 & Fig. 21). It was larger for the SD SS than for the JM SS, regardless the blend and the used setting. This substantial difference in MMAD could emerge due to a partial agglomeration of the SD SS during blending (see section 3.2.2.) and capsule filling. It could happen that sinter bridges formed between the SD SS particles, resulting in stable agglomerates [35]. These agglomerates are indeed able to detach from the carrier, but due to their large size are not able to penetrate down to the lower stages and already partly impacted in the mouthpiece and throat, as can be seen in Fig. 23. This adverse effect of particle agglomerates on the aerosolisation performance was already observed by Faulhammer et. al. [82].

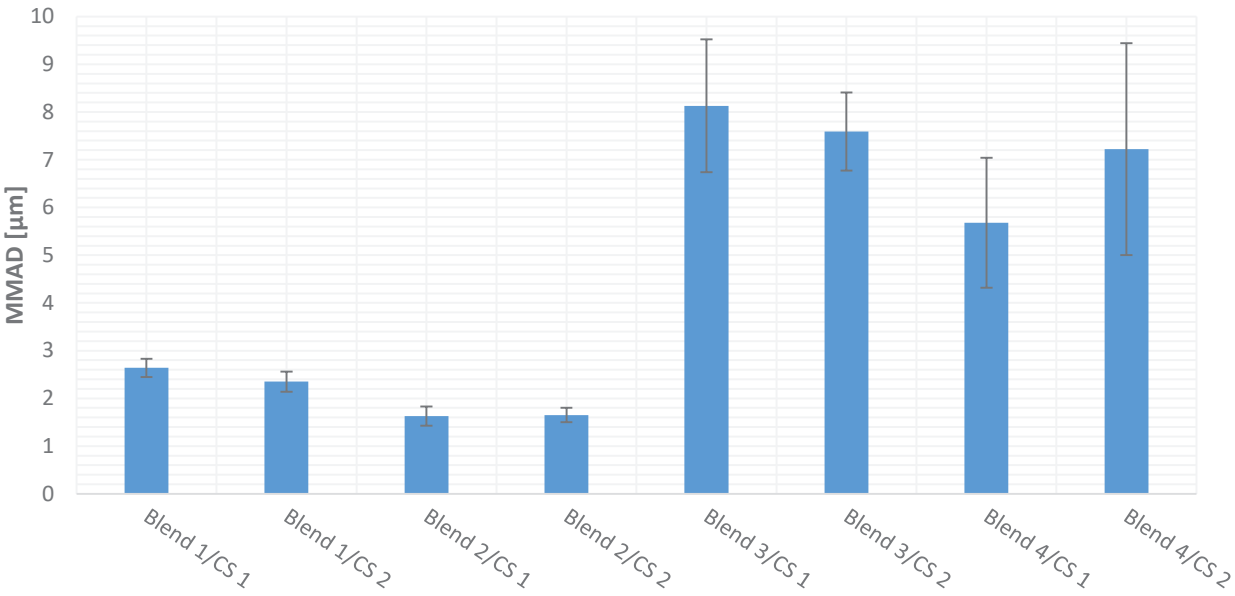

Fig. 21: MMAD of the four blends at both capsule filing settings (n=3 ± SD)

Another factor that adversely affected the FPF of the SD SS blends and which can be related to the measurements results of the MMAD, was the spherical shape of the SD SS particles. These were thereby less aerodynamic than the elongated, needle-like shaped JM SS particles. Due to that, SD SS particles had a lower capability to remain in the surrounding air

stream during inhalation and thus already impacted in the first parts of the NGI. Moreover, it might also be that a remarkable amount of SS particles, regardless if JM or SD, stayed attached to the carrier surface due to inefficient detachment forces arising during inhalation, as can be seen in the high percentage of SS that impacted in the pre-separator (Fig. 22 & 23). It could also be that partly solid bridges were formed between the SD SS particles and the carrier ones, reducing the potential of those particles to become aerosolised and thus impacted with the carrier. This phenomena was already observed by Faulhammer et. al. [36]. The interplay of the above mentioned phenomena resulted in a high amount of SD SS that already deposited in the mouthpiece, the bended inlet tube, the pre-separator or stage 1, which can be clearly seen in Fig 22 & 23. When one sums up the SS content deposited in the previously mentioned parts of the NGI, it becomes obvious that the amount of SD SS particles deposited within these four parts was higher than that one of JM SS particles. Which, in turn, resulted in the difference in FPF between the two engineered forms of the SS.

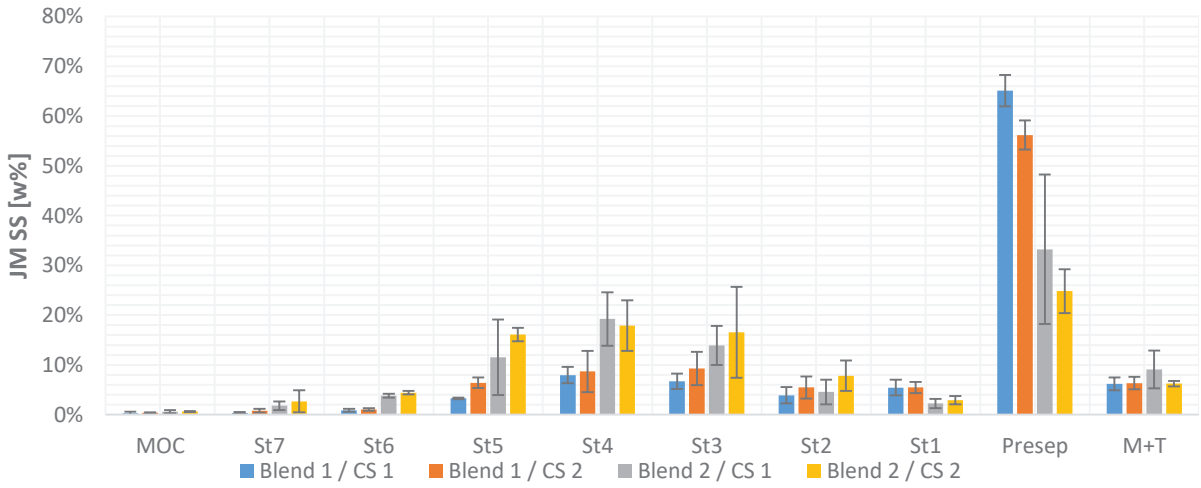

Fig. 22: Deposited amount of JM SS in w% on the individual stages of the NGI (MOC = micro-orifice collector, St1-St7 = stage 1 - 7, Presep = pre-separator and M+T = mouth piece and 90° bended inlet tube; n= 3 ± SD)

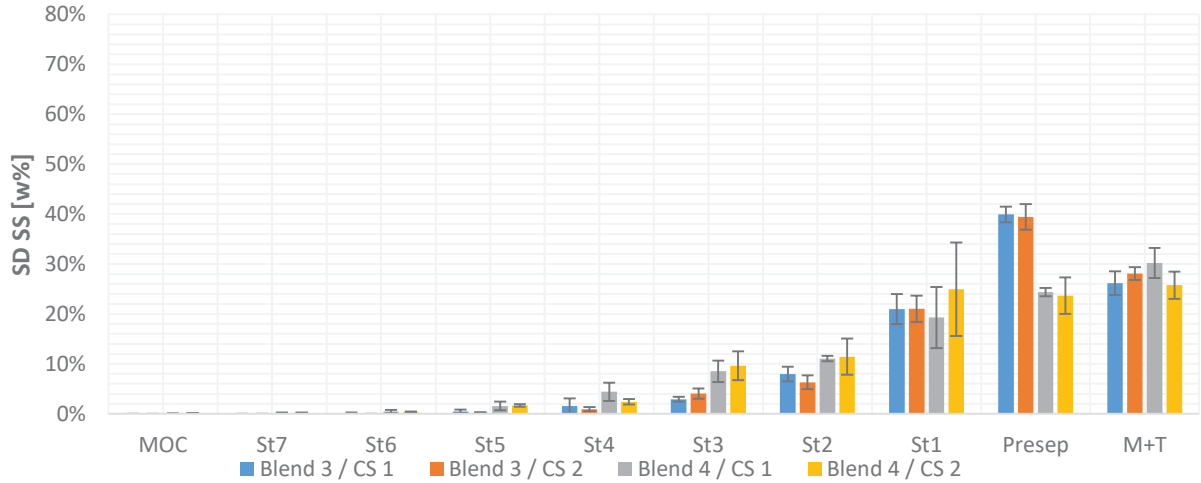

Fig. 23: Deposited amount of SD SS in w% on the individual stages of the NGI (MOC = micro-orifice collector, St1-St7 = stage 1 - 7, Presep = pre-separator and M+T = mouth piece and 90° bended inlet tube; n=3 ± SD)

Fig. 22 & 23 display an additional factor that could describe the finding that high API load blends exhibited higher FPFs than low API load ones. It is evident that most of the SS particles in the low API load blends impacted in the pre-separator. This might be explained by the fact that a high percentage of those particles was attached more tightly to the carrier surface (i.e. to active sites) and consequently was not able to detach during inhalation. Hence, they impacted with the carrier in the pre-separator, which resulted in lower FPFs. In the high API load blends, the percentage of particles attached to the active sites was much lower, since these sites were already saturated [78]. As a result, a higher amount of particles adhered more weakly and partly in layers to the carrier surface and thus got aerosolised more easily and were able to penetrate down into the lower stages of the NGI. This difference between low and high API load blends can be seen in the different amount of SS that impacted in the pre-separator.

4. Conclusion and Outlook

The two particle engineering techniques produced SS particles that differed in solid state, particle size and shape. These differences in particle physicochemical properties affected subsequently the API-carrier interaction in the produced adhesive mixtures. This greatly influenced the mixing homogeneity of the individual blends. It was explored that the screened mixing parameters provided settings that were on the one hand adequate to produce homogeneous blends with JM SS, however on the other hand, inadequate to produce homogeneous blends when SD SS was used. Moreover, it was investigated that an API load of 10% already led to a saturation of the carrier surface, resulting in loose SS particles and a partial multilayer formation of API particles on the carrier surface. As already shown by other research groups this work supported the existing knowledge that it is hard to find a mixing strategy that is generally valid, regardless of the physicochemical properties of the API, the API load or the surface structure of the carrier particles [20], [53]. This work confirms the importance of the mixing process on interactive binary DPI mixtures and supports the fact that for each form of API, each distinct API load and each API carrier combination, a mixing strategy has to be established in order to support optimal pulmonary drug administration. A prerequisite for developing such customized mixing strategies is an accurate characterisation of the physicochemical properties of the API and the carrier.

Although not all produced blends exhibited the intended mixing homogeneities, they were still used for further in vitro testing. Powder bulk characterisation showed that all blends displayed an appropriate flowability, whereas the high API load blends were more cohesive than the low API load ones. These outcomes affected also the capsule filling. In principle, all blends were suitable to fill and the achieved fill weights were approximately in the range of the target fill weight. However, the capsule fill weight variability that occurred over time in some cases, requires further investigation. To avoid this inconsistency in future research, one should take care of two things: (1) powder feeding into the dosing container of the capsule filling machine should be done automatically and not by hand and (2) a warm-up period could be implemented before capsule filling is started. The idea behind this is that within this period the densification process of the powder bed inside the rotating dosing container should be completed and a constant capsule fill weight over time could be obtained. Another thing that could be reconsidered, is the material of the used capsules. The powder retention on the HPMC capsule shells, when the powder was simply emptied, was considerable, especially when SD SS was used. As a consequence, future research work should also take into consideration the testing of new capsule materials for the application in DPIs.

Finally, the most important thing when formulating adhesive mixtures for DPIs is their aerodynamic performance. It turned out that SD SS blends performed substantially worse than JM SS blends. In summary, this inferior aerodynamic performance of the SD SS was mainly due to the interplay of some issues: (1) SD SS exhibited larger particles sizes, (2) SD SS particles formed agglomerates during processing (blending, capsule filling), (3) the SD SS particles detached insufficiently from the carrier surface due to solid bridging and (4) minor important but mentionable, the spherical shape of the SD SS adversely affected the aerodynamic properties. In future, research work should put a focus on the agglomeration and the fusion of SD SS particles during mixing and capsule filling.

Consequently, when one take all these findings, mentioned in this thesis, into account it can be finally said that JM SS are better adaptable for carrier based DPI-formulations than SD SS. It is much easier to produce, shows good API-carrier interaction, thus, it is suitable for powder blending and it generates a high FPF when it gets aerosolised. However one should also keep in mind that jet-milling offers less opportunities in terms of particle engineering and amorphous materials like SD SS could potentially display other advantages, e.g. a better dissolution performance inside the lung [83].

Appendix

A. Additional data

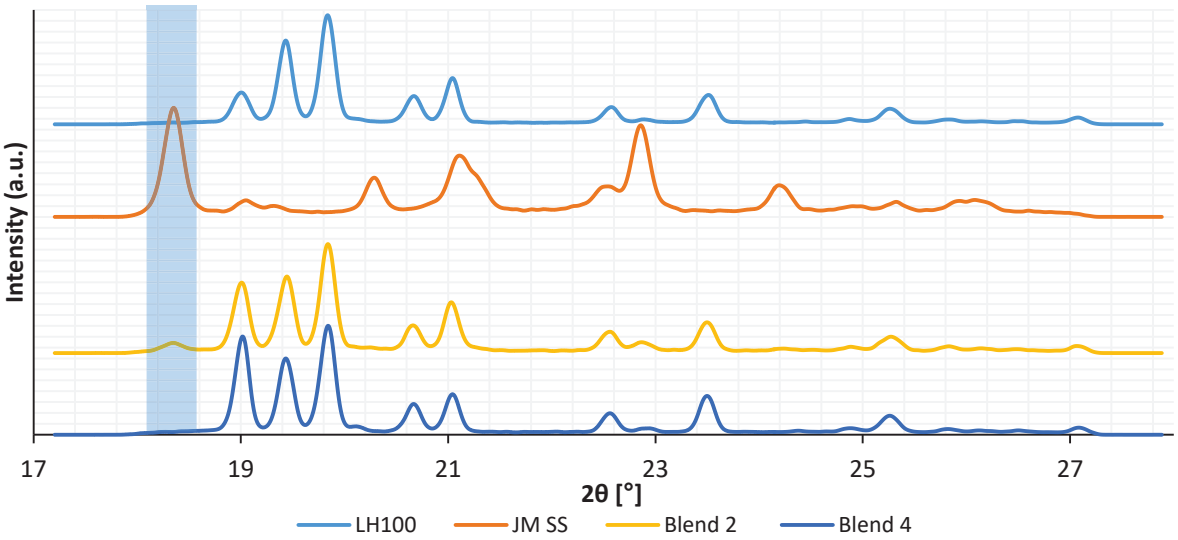

Fig. 24: WAXS pattern of blend 2 & 4 after capsule filling and as reference WAXS pattern of pure LH100 and JM SS

Tab. 17: Powder retention results of the low API load blends (n=3 ± SD)

	SS cont. total [mg]	SS cont. pow. [mg]	SS cont. Cap. [mg]	SS cont. theo. [mg]	SS cont. total / SS cont. theo. [%]	SS cont. pow. [%]	SS cont. cap. [%]
Blend 1/ M 1	271.13 ± 6.17	196.95 ± 3.01	74.28 ± 5.66	240.33 ± 4.04	112.85 ± 0.75	72.63 ± 1.55	27.37 ± 1.55
Blend 1/ M 2	209.17 ± 5.21	188.18 ± 3.13	20.99 ± 2.15	239.00 ± 4.00	87.51 ± 0.77	89.98 ± 0.77	10.02 ± 0.77
Blend 3/ M 1	238.46 ± 4.75	143.54 ± 7.30	94.92 ± 6.58	232.67 ± 7.23	102.54 ± 3.11	60.19 ± 2.69	39.81 ± 2.69
Blend 3/ M 2	183.15 ± 3.06	152.16 ± 3.83	30.99 ± 3.36	232.00 ± 1.73	78.95 ± 1.34	83.08 ± 1.77	16.92 ± 1.77

Tab. 18: Powder retention results of the high API load blends (n=3 ± SD)

	SS cont. tot. [mg]	SS cont. pow. [mg]	SS cont. cap. [mg]	SS cont. theo. [mg]	SS cont. total / SS cont. theo. [%]	SS cont. pow. [%]	SS cont. cap. [%]
Blend 2/ M 1	2598.72 ± 15.95	2311.05 ± 15.10	287.67 ± 13.59	2586.67 ± 32.15	100.47 ± 1.07	88.93 ± 0.49	11.07 ± 0.49
Blend 2/ M 2	2400.67 ± 9.50	2256.22 ± 29.41	144.45 ± 33.75	2546.67 ± 25.17	94.27 ± 1.11	93.98 ± 1.39	6.02 ± 1.39
Blend 4/ M 1	2288.03 ± 67.08	1214.63 ± 37.42	1073.40 ± 48.81	2573.33 ± 58.59	88.92 ± 2.32	53.09 ± 1.22	46.91 ± 1.22
Blend 4/ M 2	1911.77 ± 52.92	1179.62 ± 83.20	732.15 ± 38.31	2576.67 ± 25.17	74.21 ± 2.69	61.66 ± 2.83	28.34 ± 2.83

B. Bibliography

[1] B. H. J. Dickhoff, “Adhesive mixtures for powder inhalation; The effect of carrier (surface and bulk) properties, carrier payload and mixing conditions on the performance of adhesive mixtures for inhalation,” University of Groningen, Groningen, 2006.

[2] D. I. Daniher and J. Zhu, “Dry powder platform for pulmonary drug delivery,” *Particuology*, vol. 6, no. 4, pp. 225–238, 2008.

[3] N. R. Labiris and M. B. Dolovich, “Pulmonary drug delivery. Part I: Physiological factors affecting therapeutic effectiveness of aerosolized medications,” *Br. J. Clin. Pharmacol.*, vol. 56, no. 6, pp. 588–599, 2003.

[4] X. M. Zeng, G. P. Martin, and C. Marriott, “The controlled delivery of drugs to the lung,” *Int. J. Pharm.*, vol. 124, no. 2, pp. 149–164, 1995.

[5] G. Pilcer and K. Amighi, “Formulation strategy and use of excipients in pulmonary drug delivery,” *Int. J. Pharm.*, vol. 392, no. 1–2, pp. 1–19, 2010.

[6] R. U. Agu, M. I. Ugwoke, M. Armand, R. Kinget, and N. Verbeke, “The lung as a route for systemic delivery of therapeutic proteins and peptides,” *Respir. Res.*, vol. 2, no. 4, pp. 198–209, 2001.

[7] D. Traini, “Inhalation Drug Delivery,” in *Inhalation Drug Delivery: Techniques and Products*, P. Colombo, D. Traini, and F. Buttini, Eds. Chichester: John Wiley & Sons, Ltd, 2013, pp. 1–14.

[8] R. L. Johnson and C. C. W. Hsia, “Anatomy and physiology of the human respiratory system,” in *Human Respiration*, 2006, pp. 1–29.

[9] M. R. Van Scott, J. Chandler, S. Olmstead, J. M. Brown, and M. Mannie, “Airway Anatomy, Physiology, and Inflammation,” in *The Toxicant Induction of Irritant Asthma, Rhinitis, and Related Conditions*, W. J. Meggs, Ed. Boston: Springer, 2013, pp. 19–61.

[10] T. C. Carvalho, J. I. Peters, and R. O. Williams, “Influence of particle size on regional lung deposition - What evidence is there?,” *Int. J. Pharm.*, vol. 406, no. 1–2, pp. 1–10, 2011.

[11] B. H. J. Dickhoff, A. H. De Boer, D. Lambregts, and H. W. Frijlink, “The effect of carrier surface and bulk properties on drug particle detachment from crystalline lactose carrier particles during inhalation, as function of carrier payload and mixing time,” *Eur. J. Pharm. Biopharm.*, vol. 56, pp. 291–302, 2003.

[12] C. Darquenne, “Particle deposition in the lung,” in *Encyclopedia of Respiratory Medicine*, 1st ed., G. J. Laurent and S. D. Shapiro, Eds. Academic Press, 2006, pp. 300–304.

[13] H. C. Yeh, R. F. Phalen, and O. G. Raabe, “Factors Influencing the Deposition of Inhaled Particles,” *Environ. Health Perspect.*, vol. 15, pp. 147–156, 1976.

[14] B. O. Stuart, “Deposition and Clearance of Inhaled Particles,” *Environ. Health Perspect.*, vol. 55, pp. 369–390, 1984.

[15] S. Hou, J. Wu, X. Li, and H. Shu, “Practical, regulatory and clinical considerations for development of inhalation drug products,” *Asian J. Pharm. Sci.*, vol. 10, no. 6, pp. 490–500, 2015.

[16] E. Callard Preedy and P. Prokopovich, “History of inhaler devices,” in *Inhaler devices : Fundamentals, design and drug delivery*, P. Prokopovich, Ed. Cambridge: Woodhead Publishing Ltd., 2013, pp. 13–28.

[17] P. Rogliani *et al.*, “Optimizing drug delivery in COPD: The role of inhaler devices,” *Respir. Med.*, vol. 124, pp. 6–14, 2017.

[18] R. J. Malcolmson and J. K. Embleton, “Dry powder formulations for pulmonary delivery,” *Pharm. Sci. Technol. Today*, vol. 1, no. 9, pp. 394–398, 1998.

[19] W. Kaialy, A. Alhalaweh, S. P. Velaga, and A. Nokhodchi, “Influence of lactose carrier particle size on the aerosol performance of budesonide from a dry powder inhaler,” *Powder Technol.*, vol. 227, pp. 74–85, 2012.

[20] W. Kaialy, “On the effects of blending, physicochemical properties, and their interactions on the performance of carrier-based dry powders for inhalation - A review,” *Adv. Colloid Interface Sci.*, vol. 235, pp. 70–89, 2016.

[21] T. M. Crowder, J. A. Rosati, J. D. Schroeter, A. J. Hickey, and T. B. Martonen, “Fundamental Effects of Particle Morphology on Lung Delivery: Predictions of Stokes’ Law and the Particular Relevance to Dry powder Inhaler Formulation and Development,” *Pharm. Res.*, vol. 19, no. 3, pp. 239–245, 2002.

[22] A. H. De Boer, P. P. H. Le Brun, H. G. Van Der Woude, and P. Hagedoorn, “Dry powder inhalation of antibiotics in cystic fibrosis therapy, part 1: development of a powder formulation with colistin sulfate for a special test inhaler with an air classifier as de-agglomeration principle,” *Eur. J. Pharm. Biopharm.*, vol. 54, pp. 17–24, 2002.

[23] A. H. de Boer, P. Hagedoorn, M. Hoppentocht, F. Buttini, F. Grasmeijer, and H. W. Frijlink, “Dry powder inhalation: past, present and future,” *Expert Opin. Drug Deliv.*, vol. 14, no. 4, pp. 499–512, 2017.

[24] M. Y. Yang, J. G. Y. Chan, and H. K. Chan, “Pulmonary drug delivery by powder aerosols,” *J. Control. Release*, vol. 193, pp. 228–240, 2014.

[25] M. Hoppentocht, P. Hagedoorn, H. W. Frijlink, and A. H. de Boer, “Technological and practical challenges of dry powder inhalers and formulations,” *Adv. Drug Deliv. Rev.*, vol. 75, pp. 18–31, 2014.

[26] D. Prime, P. J. Atkins, A. Slater, and B. Sumby, “Review of dry powder inhalers,” *Adv. Drug Deliv. Rev.*, vol. 26, no. 1, pp. 51–58, 1997.

[27] I. Ashurst, A. Malton, D. Prime, and B. Sumby, “Latest advances in the development of dry powder inhalers,” *Pharm. Sci. Technolo. Today*, vol. 3, no. 7, pp. 246–256, 2000.

[28] D. A. Edwards, “Delivery of biological agents by aerosols,” *AIChE J.*, vol. 48, no. 1, pp. 2–6, 2002.

[29] P. Du, J. Du, and H. D. C. Smyth, “Evaluation of Granulated Lactose as a Carrier for Dry Powder Inhaler Formulations 2: Effect of Drugs and Drug Loading,” *J. Pharm. Sci.*, vol. 106, pp. 366–376, 2017.

[30] A. H. De Boer, H. K. Chan, and R. Price, “A critical view on lactose-based drug formulation and device studies for dry powder inhalation: Which are relevant and what interactions to expect?,” *Adv. Drug Deliv. Rev.*, vol. 64, no. 3, pp. 257–274, 2012.

[31] N. Islam and E. Gladki, “Dry powder inhalers (DPIs)-A review of device reliability and innovation,” *Int. J. Pharm.*, vol. 360, no. 1–2, pp. 1–11, 2008.

[32] A. H. De Boer, P. Hagedoorn, D. Gjaltema, J. Goede, and H. W. Frijlink, “Air classifier technology (ACT) in dry powder inhalation Part 1. Introduction of a novel force distribution concept (FDC) explaining the performance of a basic air classifier on adhesive mixtures,” *Int. J. Pharm.*, vol. 260, no. 2, pp. 187–200, 2003.

[33] F. Buttini, G. Colombo, P. C. L. Kwok, and W. T. Wui, “Aerodynamic assessment for inhalation products: fundamentals and current pharmacopoeial methods,” in *Inhalation Drug Delivery: Techniques and Products*, P. Colombo, D. Traini, and F. Buttini, Eds. Chichester: John Wiley & Sons, Ltd, 2013, pp. 91–119.

[34] A. J. Hickey and N. M. Concessio, “Descriptors of irregular particle morphology and powder properties,” *Adv. Drug Deliv. Rev.*, vol. 26, no. 1, pp. 29–40, 1997.

[35] J. T. Pinto, S. Radivojev, S. Zellnitz, E. Roblegg, and A. Paudel, “How does secondary processing affect the physicochemical properties of inhalable salbutamol sulphate particles? A temporal investigation,” *Int. J. Pharm.*, vol. 528, no. 1–2, pp. 416–428, 2017.

[36] E. Faulhammer, V. Wahl, S. Zellnitz, J. G. Khinast, and A. Paudel, “Carrier-based dry powder inhalation: Impact of carrier modification on capsule filling processability and in vitro aerodynamic performance,” *Int. J. Pharm.*, vol. 491, no. 1–2, pp. 231–242, 2015.

[37] A. Paudel, M. Geppi, and G. Van Den Mooter, “Structural and dynamic properties of amorphous solid dispersions: The role of solid-state nuclear magnetic resonance spectroscopy and relaxometry,” *J. Pharm. Sci.*, vol. 103, no. 9, pp. 2635–2662, 2014.

[38] W. Kaialy and A. Nokhodchi, “Particle Engineering for Improved Pulmonary Drug Delivery Through Dry Powder Inhalers,” in *Pulmonary Drug Delivery: Advances and Challanges*, 1st ed., A. Nokhodchi and G. P. Martin, Eds. John Wiley & Sons, Ltd, 2015, pp. 171–197.

[39] S. Mangal, F. Meiser, G. Tan, T. Gengenbach, D. A. V Morton, and I. Larson, “Applying surface energy derived cohesive-adhesive balance model in predicting the mixing, flow and compaction behaviour of interactive mixtures,” *Eur. J. Pharm. Biopharm.*, vol. 104, pp. 110–116, 2016.

[40] X. M. Zeng, G. P. Martin, and C. Marriott, *Particle Interactions in Dry Powder Formulations for Inhalation*. London: Taylor & Francis, 2001.

[41] P. Kulvanich and P. J. Stewart, “The effect of particle size and concentration on the adhesive characteristics of a model drug-carrier interactive system,” *J. Pharm. Pharmacol.*, vol. 39, no. 9, pp. 673–678, 1987.

[42] B. H. J. Dickhoff, M. J. H. Ellison, A. H. De Boer, and H. W. Frijlink, “The effect of budesonide particle mass on drug particle detachment from carrier crystals in adhesive mixtures during inhalation,” *Eur. J. Pharm. Biopharm.*, vol. 54, no. 2, pp. 245–248, 2002.

[43] H. Larhrib, G. P. Martin, C. Marriott, and D. Prime, “The influence of carrier and drug morphology on drug delivery from dry powder formulations,” *Int. J. Pharm.*, vol. 257, no. 1–2, pp. 283–296, 2003.

[44] D. J. Burnett, J. Khoo, M. Naderi, J. Y. Y. Heng, G. D. Wang, and F. Thielmann, “Effect of Processing Route on the Surface Properties of Amorphous Indomethacin Measured by Inverse Gas Chromatography,” *AAPS PharmSciTech*, vol. 13, no. 4, pp. 1511–1517, 2012.

[45] I. M. Grimsey, J. C. Feeley, and P. York, “Analysis of the surface energy of pharmaceutical powders by inverse gas chromatography,” *J. Pharm. Sci.*, vol. 91, no. 2, pp. 571–583, 2002.

[46] B. H. J. Dickhoff, A. H. De Boer, D. Lambregts, and H. W. Frijlink, “The interaction between carrier rugosity and carrier payload, and its effect on drug particle redispersion from adhesive mixtures during inhalation,” *Eur. J. Pharm. Biopharm.*, vol. 59, no. 1, pp. 197–205, 2005.

[47] P. M. C. Lacey, “The mixing of solid particles,” *Chem. Eng. Res. Des.*, vol. 75, pp. 49–55, 1997.

[48] J. A. Hersey, “Ordered mixing: A new concept in powder mixing practice,” *Powder Technol.*, vol. 11, no. 1, pp. 41–44, 1975.

[49] J. N. Staniforth, “Total mixing,” *Int. J. Pharm. Tech. Prod. Mfr. 2*, pp. 7–12, 1981.

[50] J. N. Staniforth, “Order out of chaos,” *J. Pharm. Pharmacol.*, vol. 39, no. 5, pp. 329–334, 1987.

[51] T. Yin, “A guide to blend uniformity,” *J. GXP Compliance*, vol. 12, no. 1, pp. 46–51, 2007.

[52] S. Sarkar, B. Minatovicz, K. Thalberg, and B. Chaudhuri, “Development of a Rational Design Space for Optimizing Mixing Conditions for Formation of Adhesive Mixtures for Dry-Powder Inhaler Formulations,” *J. Pharm. Sci.*, vol. 106, no. 1, pp. 129–139, 2017.

[53] D. Nguyen, A. Rasmuson, I. Niklasson Björn, and K. Thalberg, “Mechanistic time scales in adhesive mixing investigated by dry particle sizing,” *Eur. J. Pharm. Sci.*, vol. 69, pp. 19–25, 2015.

[54] B. Chaudhuri, A. Mehrotra, F. J. Muzzio, and M. S. Tomassone, “Cohesive effects in powder mixing in a tumbling blender,” *Powder Technol.*, vol. 165, pp. 105–114, 2006.

[55] Food and Drug Administration, “Guidance for Industry, Powder Blend and Finished Dosage Units - Stratified In-Process Dosage Unit Sampling and Assessment,” 2003.

[56] T. Garcia *et al.*, “Recommendations for the Assessment of Blend and Content Uniformity: Modifications to Withdrawn FDA Draft Stratified Sampling Guidance,” *J. Pharm. Innov.*, vol. 10, no. 1, pp. 76–83, 2014.

[57] U. V Shah, V. Karde, C. Ghoroi, and J. Y. Y. Heng, “Influence of particle properties on powder bulk behaviour and processability,” *Int. J. Pharm.*, vol. 518, no. 1–2, pp. 138–154, 2017.

[58] T. Freeman, “Powder characterisation for inhaled drug delivery,” *Freemantechnology*, pp. 1–9, 2011.

[59] F. Podczeck, “Powder, granule and pellet properties for filling of two-piece hard capsules,” in *Pharmaceutical Capsules*, 2nd ed., F. Podczeck and B. E. Jones, Eds. Pharmaceutical Press, 2004, pp. 101–118.

[60] P. M. Young, O. Wood, J. Ooi, and D. Traini, “The influence of drug loading on formulation structure and aerosol performance in carrier based dry powder inhalers,” *Int. J. Pharm.*, vol. 416, no. 1, pp. 129–135, 2011.

[61] D. Edwards, “Applications of capsule dosing techniques for use in dry powder inhalers,” *Ther. Deliv.*, vol. 1, no. 1, pp. 195–201, 2010.

[62] F. Podczeck, “Dry filling of hard capsules,” in *Pharmaceutical Capsules*, 2nd ed., F. Podczeck and B. E. Jones, Eds. Pharmaceutical Press, 2004, pp. 119–138.

[63] SaintyCo, “Working Principle of Dosator Type Capsule Filling Machine to Filling Powder into Low Fill Weight Capsules.” [Online]. Available: http://www.saintytec.com/dosator-type-capsule-filling-machine/. [Accessed: 16-Oct-2017].

[64] E. Faulhammer *et al.*, “Low-dose capsule filling of inhalation products: critical material attributes and process parameters,” *Int. J. Pharm.*, vol. 473, no. 1–2, pp. 617–626, 2014.

[65] U. S. Pharmacopeia, “Aerosols, nasal sprays, metered-dose inhalers, and dry powder inhalers.”

[66] Copley Scientific, “Quality Solutions for Inhaler Testing,” 2015.

[67] M. Taki, C. Marriott, X. Zeng, and G. P. Martin, “Aerodynamic deposition of combination dry powder inhaler formulations in vitro: A comparison of three impactors,” *Int. J. Pharm.*, vol. 388, pp. 40–51, 2010.

[68] D. Brone, A. Alexander, and F. J. Muzzio, “Quantitative Characterization of Mixing of Dry Powders in V-Blenders,” *AIChE J.*, vol. 44, no. 2, pp. 271–278, 1998.

[69] FreemanTechnology, “FT4 Support documents - Methodologies.”

[70] S. Stranzinger *et al.*, “The effect of material attributes and process parameters on the powder bed uniformity during a low-dose dosator capsule filling process,” *Int. J. Pharm.*, vol. 516, no. 1–2, pp. 9–20, 2017.

[71] J. H. Kirk, S. E. Dann, and C. G. Blatchford, “Lactose: A definitive guide to polymorph determination,” *Int. J. Pharm.*, vol. 334, no. 1–2, pp. 103–114, 2007.

[72] S. A. F. ad S. Muhammad *et al.*, “A novel method for the production of crystalline micronised particles,” *Int. J. Pharm.*, vol. 388, no. 1–2, pp. 114–122, 2010.

[73] S. Zellnitz, O. Narygina, C. Resch, H. Schroettner, and N. A. Urbanetz, “Crystallization speed of salbutamol as a function of relative humidity and temperature,” *Int. J. Pharm.*, vol. 489, no. 1–2, pp. 170–176, 2015.

[74] X. M. Zeng, K. H. Pandhal, and G. P. Martin, “The influence of lactose carrier on the content homogeneity and dispersibility of beclomethasone dipropionate from dry powder aerosols,” *Int. J. Pharm.*, vol. 197, no. 1–2, pp. 41–52, 2000.

[75] H. Larhrib, X. M. Zeng, G. P. Martin, C. Marriott, and J. Pritchard, “The use of different grades of lactose as a carrier for aerosolised salbutamol sulphate,” *Int. J. Pharm.*, vol. 191, no. 1, pp. 1–14, 1999.

[76] E. M. Littringer, R. Paus, A. Mescher, H. Schroettner, P. Walzel, and N. A. Urbanetz, “The morphology of spray dried mannitol particles - The vital importance of droplet size,” *Powder Technol.*, vol. 239, pp. 162–174, 2013.

[77] F. Grasmeijer, P. Hagedoorn, H. W. Frijlink, and H. A. De Boer, “Mixing Time Effects on the Dispersion Performance of Adhesive Mixtures for Inhalation,” *PLoS One*, vol. 8, no. 7, pp. 1–18, 2013.

[78] F. Grasmeijer, P. Hagedoorn, H. W. Frijlink, and A. H. de Boer, “Drug Content Effects on the Dispersion Performance of Adhesive Mixtures for Inhalation,” *PLoS One*, vol. 8, no. 8, pp. 1–12, 2013.

[79] L. J. Jallo, C. Ghoroi, L. Gurumurthy, U. Patel, and R. N. Davé, “Improvement of flow and bulk density of pharmaceutical powders using surface modification,” *Int. J. Pharm.*, vol. 423, no. 2, pp. 213–225, 2012.

[80] F. Podczeck and Y. Miah, “The influence of particle size and shape on the angle of internal friction and the flow factor of unlubricated and lubricated powders,” *Int. J. Pharm.*, vol. 144, no. 2, pp. 187–194, 1996.

[81] E. Cordts and H. Steckel, “Capabilities and limitations of using powder rheology and permeability to predict dry powder inhaler performance,” *Eur. J. Pharm. Biopharm.*, vol. 82, no. 2, pp. 417–423, 2012.

[82] E. Faulhammer, S. Zellnitz, T. Wutscher, S. Stranzinger, A. Zimmer, and A. Paudel, “Performanc indicators for carrier based DPIs: Carrier surface properties for capsule filling and API properties for in vitro aerosolisation,” *Int. J. Pharm.*, 2017.

[83] H. X. Ong, D. Traini, M. Bebawy, and P. M. Young, “Epithelial profiling of antibiotic controlled release respiratory formulations,” *Pharm. Res.*, vol. 28, no. 9, pp. 2327–2338, 2011.

C. List of tables

D. List of figures

E. List of abbreviations

d	Characteristic diameter
d_{50}	Cut-off diameter of the NGI stages
d_{AE}	Aerodynamic diameter
d_P	Particle diameter
μ	Dynamic viscosity
ρ_0	Density that equals unity
ρ_P	Density of the particle
Δp	Pressure drop
Q	Flow rate through the NGI
u	Velocity of the air stream
χ	Shape factor of the particle
$d_{v,}x$	Volume equiv. diameter, where x% of the PSD possess a smaller diameter.
AE	Aerated energy
AIF	Angle of internal friction
API	Active pharmaceutical ingredient
AR	Aeration ratio
BFE	Basic flowability energy
CFS	Capsule fill setting
DPI	Dry powder inhaler
ED	Emitted dose
FFC	Flow function coefficient
FPD	Fine particle dose
FPF	Fine particle fraction
HPLC	High-performance liquid chromatography
HPMC	Hydroxypropyl-methylcellulose
JM	Jet milled
LH100	Lactohale 100
MC	Mixing condition
MMAD	Mass median aerodynamic diameter
MOC	Micro-orifice collector
NGI	Next generation impactor
pMDI	Pressurized metered-dose inhaler
PSD	Particle size distribution
RSD	Relative standard deviation
RFR	Reduced filling ratio
rpm	Rounds per minute
SD	Spray dried
SEM	Scanning electron microscopy
SS	Salbutamol sulphate
SWAXS	Small and wide angle X-ray scattering